Published in final edited form as:
Dev Biol. 2004 December 15; 276(2): 523–540. doi:10.1016/j.ydbio.2004.09.020.

dlx3b and *dlx4b* function in the development of Rohon-Beard sensory neurons and trigeminal placode in the zebrafish neurula

Takao Kaji and **Bruk Artinger***
Department of Craniofacial Biology, University of Colorado Health Sciences Center, Denver, CO 80262, USA

Abstract

Rohon-Beard sensory neurons, neural crest cells, and sensory placodes can be distinguished at the boundary of the embryonic epidermis (skin) and the neural plate. The inductive signals at the neural plate border region are likely to involve a gradient of bone morphogenic protein (BMP) in conjunction with FGF and Wnts and other signals. However, how these signals are transduced to produce the final cell fate remains to be determined. Recent evidence from *Xenopus* and chick suggest that *Dlx* genes are required for the generation of cell fates at the neural plate border (McLarren, K.W., Litsiou, A., Streit, A., 2003. DLX5 positions the neural crest and preplacode region at the border of the neural plate. Dev. Biol. 259, 34–47; Woda, J.M., Pastagia, J., Mercola, M., Artinger, K.B., 2003. Dlx proteins position the neural plate border and determine adjacent cell fates. Development 130, 331–342). In the present study, we extend these findings to zebrafish, where we unequivocally demonstrate that *dlx3b* and *dlx4b* function in a dose-dependent manner to specify cell fates such as Rohon-Beard sensory neurons and trigeminal sensory placodes. *dlx* function was examined by inhibiting: (1) protein levels with antisense morpholino oligonucleotides (MOs), and (2) activity by repressing the ability of dlx-homeodomain to bind to downstream targets (*EnR-dlx3bhd* mRNA; dlx3b homeodomain fused to Engrailed transcriptional repressor domain). Inhibition of dlx3b and dlx4b protein and activity resulted in the reduction or complete loss of Rohon-Beard (RB) sensory neurons and trigeminal (TG) sensory placodes. These data suggest that *dlx3b* and *dlx4b* function in the specification of RB neurons and trigeminal sensory placodes in zebrafish. Further, we have shown that *dlx3b* and *dlx4b* function in a non-cell-autonomous manner for RB neuron development; *dlx3b* and *dlx4b* act to regulate *bmp2b* expression at the non-neural ectodermal border. These data suggest that the contribution of *dlx3b* and *dlx4b* to neural plate border formation is partially non-cell-autonomous acting via BMP activity.

Keywords

dlx genes; *bmp* genes; Neural crest; Rohon-Beard sensory neurons; Sensory placodes; Neural plate

*Corresponding author. Department of Craniofacial Biology, University of Colorado Health Sciences Center, 4200 East Ninth Avenue, Denver, CO 80262. Fax: +1 303 315 3013. Kristin.Artinger@uchsc.edu (K.B. Artinger).

Introduction

In zebrafish and *Xenopus laevis*, neural crest, Rohon-Beard (RB) neurons, and placodes arise along the neural plate border during neurula stage (Baker and Bronner-Fraser, 2001; Bally-Cuif and Hammerschmidt, 2003). Specification of cells at the neural plate border is thought to be mediated by inductive signals, including BMPs, FGFs, and Wnts, from the adjacent non-neural ectoderm during gastrula and neurula stages (Aybar and Mayor, 2002). In dorsoventral pattern formation of *Xenopus* gastrulae, Noggin, Chordin, and Follistatin proteins, secreted from the Spemann organizer, bind BMP4 in the dorsal region and prevent it from binding its receptor. Near the organizer, BMP4 is strongly inhibited by Noggin, Chordin, and Follistatin, which causes the specification of the neural plate. Inhibition gradually becomes weaker in the regions more distant from the organizer, such that intermediate levels of BMP signaling specify cell fate at the neural plate border. At a greater distance, there is little or no inhibition, which results in the specification of the epidermis. In zebrafish, the existence of a similar mechanism has been suggested, which was revealed by observations in embryos exhibiting dorsoventral axis defects (Nguyen et al., 1998, 2000).

In *Xenopus* and chick, *Dlx3* and *Dlx5*, members of *distal-less* family of homeobox genes, are broadly expressed in the non-neural ectoderm adjacent to the neural plate, where *BMP4* also is expressed, between early gastrula stage and neurula stage (Feledy et al., 1999; Pera et al., 1999). From their gene expression patterns, it was suggested that there is a regulatory relationship between *Dlx* genes and *BMP4*, and that the *Dlx* genes can act to promote epidermis and to repress neural plate development. Recent studies concerning *Dlx* gene function suggest that these transcription factors affect neural crest, RB neuron, and placodal development, as well as neural plate-border positioning (McLarren et al., 2003; Woda et al., 2003). In zebrafish, there are 8 *dlx* genes (Panganiban and Rubenstein, 2002). Among them, 6 *dlx* genes constitute three chromosomally linked pairs, and the remaining 2, *dlx2b* and *dlx4a*, are not linked to each other. The expression of two of these genes, *dlx3b* and *dlx4b*, is in the non-neural ectoderm adjacent to the neural plate at an early embryonic stage, and is similar to those of *Xenopus Dlx3* and chick *Dlx5*. The other *dlx* genes in zebrafish are not expressed in this region. It has been suggested that *dlx3b* and *dlx4b* have cross-regulatory interactions between them and that they function in the development of otic and olfactory placodes (Liu et al., 2003; Solomon and Fritz, 2002). Further, our data from experiments in *Xenopus* suggest that *Dlx* genes play a role in specifying neural plate border fates. However, we consider these data equivocal, since we primarily used artificial constructs in which a large Engrailed repressor (EnR) was attached to the homeodomain of Dlx3b. We do not know, for example, if this large repressor domain is interfering with transcription of non-Dlx targets. To determine the role of *dlx* genes unequivocally, we have turned to a Morpholino-based knockdown in zebrafish and directly compared these data to the EnR–Dlx3b homeodomain injected embryos. Thus, we describe the function of *dlx3b* and *dlx4b* in zebrafish neurula, specifically looking at RB neuron, trigeminal placodal development, in addition to neural plate and neural crest development.

Two loss-of-function strategies were employed to investigate *dlx3b* and *dlx4b* function in zebrafish: morpholino antisense oligonucleotides to the translation start site (ATG) as well as directed to the exon2/intron2 splice site (E2I2), and a construct where dlx3b

homeodomain is fused to Engrailed transcriptional repressor domain. We find that the marker-gene-expression of RB neurons and trigeminal placodes was highly reduced or absent, that of neural crest was slightly reduced, and that of neural plate was slightly broadened, in the embryos injected with MOs or *EnR-dlx3bhd* mRNA. Further, among *bmp* genes, a reduction of *bmp2b* gene-expression occurred at the non-neural ectodermal border in embryos at 90% epiboly, and RB neuron development was affected by non-cell-autonomous action of *dlx3b* and *dlx4b*. These findings suggest that *dlx3b* and *dlx4b* are required in RB neuron and trigeminal placodal development, and that some of the defects attributable to reduction of these *dlx* gene products are likely to be caused by the reduction of *bmp2b* expression.

Materials and methods

Antisense morpholino oligonucleotide

An antisense morpholino oligonucleotide (MO) having the sequence 5′-TATGTCGGTCCACTCATCCTTAATA-3′ was designed to target *dlx3b* mRNA, and a MO having the sequence 5′ATAGACATCATTAACCGTCAAGTCC-3′ was designed to target *dlx4b* mRNA (Gene Tools, LLC). These bind the AUG translation initiation site of *dlx3b* and *dlx4b* mRNA. Two additional MOs were made to bind the exon2/intron2 splice site (E2I2) of *dlx3b* and *dlx4b* nuclear RNA. The *dlx3b* E2I2 MO sequence was 5′-AGGTGTACCTGTGTCTGTGTGAGCC-3′ and the *dlx4b* E2I2 MO sequence was 5′-TGATGGATATTTACCTGTGTTTGCG-3′. An MO having the sequence 5′CCTCTTACCTCAGTTACAATTTATA-3′ was used as a control MO. The oligonucleotides were dissolved in distilled water. Eight to 20 ng *dlx3b*-MO and 8–20 ng *dlx4b*-MO were simultaneously injected into the yolk of 1- to 8-cell-stage embryos together with 10 kMW lysinated fluorescein dextran (LFD) or 10 kMW lysinated tetramethylrhodamine dextran (LRD) (Molecular Probes) for a total volume of 10–20 nl. Control MO of 40 ng in 10–20 nl was also injected in some experiments.

RT-PCR

Total RNA of wild type or 20 ng *dlx3b* E2I2 MO/20 ng *dlx4b* E2I2 MO injected embryos at 90% epiboly or 2–3-somite stage was isolated by using the RNAqueous kit (Ambion). In each case, about 20 embryos were used. First-strand cDNA was synthesized with total RNA, 300 ng of oligo dT primer, 200 units of SuperScriptII Reverse Transcriptase (Invitrogen), 1 mM dNTP, first strand buffer, 0.01 mM DTT, and 40 units of RNase Inhibitor, and incubated at 42°C for 50 min. PCR was performed with a forward primer in exon1 (5′-TGAGTGGACCGACATATGACA-3′) and a reverse primer in exon3 (5′-TTAATACACGGCCCCCACG-3′) of *dlx3b*, and with a forward primer in exon1 (5′-GTACACGGATTGCACTCA-3′) and a reverse primer in exon3 (5′-CAGTGGCCGTAATTGTTCAT-3′) of *dlx4b*.

Whole-mount in situ hybridization and immunohistochemistry

The following DIG or fluorescein-labeled antisense RNA probes (Roche Diagnostics) were used for in situ hybridization: *axial* (Strähle et al., 1993), *bmp2b* (Kishimoto et al., 1997), *bmp4* (Nikaido et al., 1997), *bmp7* (Dick et al., 2000), *dlx3b* (Ekker et al., 1992), *gsc*

(Schulte-Merker et al., 1994a), *HuC* (Kim et al., 1996), *isl-1* (Appel et al., 1995), *krx20* (Oxtoby and Jowett, 1993), *neuroD* (Blader et al., 1997), *neurogenin1* (Blader et al., 1997), *ntl* (Schulte-Merker et al., 1994b), *paraxis* (Shanmugalingam and Wilson, 1998), *pax2a* (Krauss et al., 1991), and *tlx3a* (Langenau et al., 2002). Single color whole-mount in situ hybridization was performed as described by Thisse and Thisse (1998). Two-color whole-mount in situ hybridization was performed essentially as described by Sawada et al. (2000). When MOs were injected into the yolk of the embryos for two-color in situ hybridization, LRD was used as a tracer. First color staining was performed with Fast Red (Roche), and second color staining was with NBT/BCIP (SIGMA), in two-color in situ hybridization.

A polyclonal antibody, anti-Dll (Panganiban et al., 1995) was used at the dilution 1:100. Immunohistochemistry was performed as described by Solnica-Krezel and Driever (1994).

Trypan blue staining

Wild type, 20 ng ATG *dlx3b*-MO- and 20 ng ATG *dlx4b*-MO-injected, and 40 ng control MO-injected embryos at 2–3-somite stage were put in 0.2 mg/ml trypan blue (SIGMA) in egg water, and left for 30 min at room temperature. Embryos were then rinsed two times in phosphate-buffered saline (PBS), and fixed in 4% paraformaldehyde (PFA) in PBS overnight. To get blue-stained pattern in embryos as positive control, a tungsten needle or a forcep was used to damage the membranes of cells in wild-type 2-somite-stage embryos, and the embryos were stained.

Constructs and RNA injections

pCS2-*EnR-dlx3bhd* and pCS2-*VP16-dlx3bhd* were previously described (Woda et al., 2003). Capped RNAs were produced by using the mMessage mMachine kit (Ambion). *EnR-dlx3bhd* mRNA (60–200 pg) was injected into the cell of 1-cell-stage embryos together with 10 kMW LFD (Molecular Probes) totally in 3–6 nl. In the rescue experiment, *VP16-dlx3bhd* mRNA (150 pg) was at first injected into the cell of 1-cell-stage embryos together with 10 kMW LFD in 3–6 nl, and next *dlx3b/dlx4b* ATG MO was injected into the yolk between 1- and 4-cell stage.

Cell transplantation

Mosaic embryos were generated as described by Schier et al. (1997). At first, the mosaic embryos, where labeled MO-injected cells are in host wild-type embryos, were made. Donor cells were removed from the epiblasts of the donor embryos; mid-blastula embryos which were injected with 20 ng ATG *dlx3b*-MO/20 ng ATG *dlx4b*-MO and 5% lysinated fluorescein/biotin dextran (10 kMW, Molecular Probes) into the yolk at 1- to 4-cell stage. Twenty to 40 donor cells were placed into the epiblast of each host embryo, an unlabeled wild-type mid-blastula embryo. The embryos were allowed to develop until 3-somite stage, and fixed in 4% PFA in PBS. Then, whole-mount in situ hybridization was performed using *HuC* probe, and a peroxidase reaction was done after using the ABC-peroxidase kit (Vector Laboratories, Inc.). Donor cells appeared as brown-stained cells. Next, the mosaic embryos, where labeled wild-type cells are in host MO-injected embryos, were made. Donor cells were removed from the epiblasts of the wild-type mid-blastula embryos, which were injected with fluorescein/biotin dextran into the yolk. The donor cells were put into the

epiblasts of MO-injected mid-blastula embryos. Then, analyses were done as in the case with the host wild-type embryos having labeled donor MO-injected cells.

Zebrafish maintenance and strain

The wild-type zebrafish strain used in this study was AB/TL, and maintained according to Westerfield (1993).

Results

dlx3b-MO and dlx4b-MO deplete dlx proteins or alter splicing in MO-injected embryos

To examine the role of *dlx3b* and *dlx4b* in the development of the border between neural and non-neural ectoderm in zebrafish neurula, morpholino antisense oligonucleotides, which specifically target transcripts of *dlx3b* and *dlx4b* and inhibit their translation or proper splicing were generated (hereafter referred to as *dlx3b*/*dlx4b*-ATG-MOs or E2I2-MOs, respectively; Draper et al., 2001; Nasevicius and Ekker, 2000). Morpholinos, as well as a fluorescein dextran (LFD) or a rhodamine dextran (LRD) as a tracer, were injected into the yolk of 1- to 8-cell-stage embryos, and phenotypes were examined at 11 and 12.5 hpf. First of all, to examine whether *dlx3b*/*dlx4b*–ATG-MOs deplete dlx3b and dlx4b proteins specifically and effectively in embryos, whole-mount immunostaining with a polyclonal antibody against butterfly Dll homeodomain (Panganiban et al., 1995) was performed on 20 ng *dlx3b*–ATG-MO- and 20 ng *dlx4b*–ATG-MO-injected embryos. It was revealed that dlx3b and dlx4b proteins were lost in early stage embryos.

In wild-type embryos at late blastula stage, anti-Dll expression is seen in the entire epiblast (data not shown). We unexpectedly found an embryo that had a partial dispersion of MOs in the epiblast (Fig. 1A). We considered that the dispersion of MOs corresponded to that of the fluorescence (LFD) in the embryo. Fortuitously, the delay of injection (8-cell stage) appears to cause the partial dispersion of MO/LFD, allowing us to visualize where the MO is active. In the epiblast of that embryo, the anti-Dll-stained region and the MO-dispersed region were clearly complementary (Figs. 1A and B). At 6-somite stage, anti-Dll immunoreactivity was compared between wild-type and MO-injected embryos. In wild-type embryos, anti-Dll labeling could be seen in the otic placodal primordium, which is outside the central nervous system at the level of the hindbrain (Figs. 1C and E, arrowhead). In MO-injected embryos, anti-Dll labeling was extremely reduced or absent (Fig. 1D). *dlx3b* is expressed in the epiblast of late blastulae, and *dlx3b* and *dlx4b* are expressed in the otic placodal primordium at 6-somite stage (not shown). These results of late blastula stage and 6-somite stage suggest that *dlx3b*-MO and *dlx4b*-MO deplete specifically dlx3b and dlx4b protein, respectively, in embryos. The other zebrafish *dlx* genes are not expressed in the region of the neural plate border, and thus were not considered in this study.

A second set of *dlx3b/dlx4b* MOs that disrupt splicing in nuclear RNA were also used in this study (now referred to as *dlx3b/dlx4b*-E2I2-MOs). Splice blocking MOs have been used in zebrafish as an alternative method to knockdown gene function by disrupting proper splicing of RNA (Draper et al., 2001). We designed MOs that disrupt splicing for both *dlx3b* and *dlx4b* in the exon2–intron2 boundary of each, which would result in a reduction in size of

exon2. This is the exon that contains a large part of the homeodomain, and the splice block MOs at exon2–intron2 would reduce the size of the homeodomain by 72% for dlx3b and by 75% for dlx4b. A reduction in size of 185 bp for *dlx3b* and 194 bp for *dlx4b* was predicted. The effect of the 20 ng *dlx3b*/20 ng *dlx4b* E2I2-MOs on splicing was observed by isolation of embryos injected with *dlx3b/dlx4b*-E2I2-MOs at the 1- to 4-cell stage, isolating RNA from non-injected control and *dlx3b/dlx4b*-E2I2-MO-injected embryos at 2–3-somite stage and 90% epiboly, synthesizing first-strand cDNA, and performing RT-PCR for *dlx3b* and *dlx4b*. Embryos injected with the *dlx3b/dlx4b*-E2I2-MOs had the mis-splicing in *dlx3b/dlx4b* as compared to a wild-type control (Fig. 1F). In *dlx4b*, we observed the expected splice variant, where we observed an approximate reduction of 200 bp, suggesting that mis-splicing occurred at the exon2–intron2 boundary. For *dlx3b*, we observed two forms of mis-spliced mRNA: one form which had approximately 180 bp deleted, as predicted, and another splice variant which had a 100-bp increase in size. Sequence analysis of the latter larger fragment confirmed that it had a 137-bp reduction of the 3′ end of exon2, consistent with the MO binding to this site and interfering with splicing, and in addition had a portion of intron2 attached. Thus, an increase in size of approximately 100 bp was observed in the larger fragment. This suggests that mis-splicing did occur. At 90% epiboly, complete splicing did occur, as shown by the presence of the sharp band at 630 bp (Fig. 1F, 90% epiboly E2I2+RT lane bottom panel). Although there is a wild-type *dlx3b* mRNA produced at 2- to 3-somite stage, we feel that sufficient mis-splicing has occurred to explain the observed phenotypes, since at around 90% epiboly, we feel *dlx3b* is acting to pattern the neural plate border. We have used both the ATG and E2I2 *dlx3b/dlx4b* MOs in this study, with the majority of the analysis with the ATG MOs. The observation that both the dll protein levels and the splicing of *dlx3b* and *dlx4b* are defective suggests that the effects on RB neurons and trigeminal placode described below are specific to depletion of dlx3b/dlx4b protein or the creation of a non-functioning protein.

dlx3b and dlx4b are required for Rohon-Beard sensory neuron development

HuC and *isl-1* are expressed in all primary neurons at early stages of neural development in zebrafish (Kim et al., 1996; Korzh et al., 1993). In addition, RB neurons at 3-somite stage express a homeobox gene, *tlx3a* (Langenau et al., 2002). In *nrd* mutant zebrafish, which lack RB neurons, *tlx3a* expression is absent (Artinger et al., 1999).

To investigate the role of *dlx3b* and *dlx4b* in RB neuron development, the expression of *HuC*, *tlx3a* and *isl-1* were studied in ATG and E2I2 *dlx3b*-MO- and *dlx4b*-MO-injected embryos by whole-mount in situ hybridization at 3- and 6-somite stage. The expression of *HuC* and *tlx3a* in RB neurons was significantly reduced or absent as compared to wild-type embryos at 3-somite stage (Figs. 2B, C, G, H compare with wild type in 2A and F; Table 1). To confirm the function of *dlx* genes which are expressed during early embryonic stages, we also injected approximately 150 pg *EnR-dlx3bhd* mRNA into the cell of 1-cell-stage embryos. The expression of *HuC and tlx3a* were examined by in situ hybridization. Phenotypes seen were very similar to those in *dlx3b*-MO- and *dlx4b*-MO-injected embryos. In the *EnR-dlx3bhd* mRNA injected embryos, *HuC and tlx3a* expression marking RB neurons could not be detected (Figs. 2D and I as compared to wild type in 2A and F). Control MO-injected embryos at the same concentration are also shown for *HuC* and *tlx3a*

(Figs. 2E and J). These results suggest that dlx activity as mediated through dlx3b and dlx4b is required in RB neuron development.

To determine if the effects are maintained over a longer period of development, we assayed both the expression of *HuC* and *isl-1* at a slightly later stage, 6-somites, in *dlx3b*-MO- and *dlx4b*-MO-injected embryos (see Fig. 5 about *isl-1* phenotype at 3-somite stage). Consistent with earlier results, we observed a reduction in the number of RB neurons with both *isl-1* and *HuC* (Figs. 2L and N as compared to 2K and M). In a higher magnification view of *dlx3b*-MO- and *dlx4b*-MO-injected embryos, the reduction of RB neurons can be easily visualized (Fig. 2P compared with 2O).

In addition to RB neurons, other cell types exist at the border of the neural plate, including neural crest cells. Both neural plate and neural crest formation was assayed with *kheper* and *fkd6* (Muraoka et al., 2000; Odenthal and Nüsslein-Volhard, 1998). Slight widening of the neural plate and reduction of neural crest was observed (see wider neural plate in Fig. 2L as compared to 2K; and data not shown). These results suggest that *dlx3b* and *dlx4b* are required for RB neuron development, and may play a role in the positioning of other cells at the neural plate border, including neural crest cells.

dlx3b and dlx4b are required for trigeminal placodal development

In the trigeminal placodes of 3-somite-stage zebrafish embryos and *Xenopus* neurulae, *neuroD* is expressed (Blader et al., 1997; Schlosser and Northcutt, 2000); in otic placodal primordia at 3-somite stage, *pax2a* is expressed (Krauss et al., 1991). In zebrafish, *neuroD* expression is lost in *neurogenin1*-MO-injected embryos, which develop no trigeminal placodes (Andermann et al., 2002). In *Pax2*-deficient mice, the development of the inner ear becomes incomplete (Torres et al., 1996).

In order to investigate the effects of *dlx3b*-MO and *dlx4b*-MO on trigeminal placodal development, we assayed the expression of *HuC*, *neuroD/pax2a*, and *isl-1* in ATG and E2I2 *dlx3b*-MO- and *dlx4b*-MO-injected embryos at 3- and 6-somite stage. Expression of *HuC* and *neuroD*/*pax2a* in the trigeminal placode was extremely reduced or absent as compared to wild-type embryos at 3-somite stage (Figs. 3B and C as compared to 3A and Figs. 3G and H as compared to 3F; Table 1). Consistent with the results reported by Solomon and Fritz (2002), the expression of *pax2a* marking otic placodal primordia was lost (Figs. 3G and H). *neuroD* expression, as well as *pax2a* expression, in the placodal primordial region, which is outside the anterior central nervous system, was extremely reduced or absent (Figs. 3G and H).

To confirm the function of *dlx* genes on trigeminal placodal development, we also injected approximately 150 pg *EnR-dlx3bhd* mRNA into the cell of 1-cell-stage embryos. The expression of *HuC* and *neuroD/pax2a* at 3-somite stage was examined by in situ hybridization. Phenotypes seen were very similar to those in *dlx3b*-MO- and *dlx4b*-MO-injected embryos. In the *EnR-dlx3bhd* mRNA injected embryos, *HuC and neuroD/pax2a* expression was highly reduced or absent in the placodal primordial region (Figs. 3D and I as compared to wild type in 3A and F). Control MO-injected embryos at the same concentration are also shown for *HuC* and *neuroD/pax2a* (Figs. 3E and J). These results

suggest that dlx activity as mediated through dlx3b and dlx4b is required in trigeminal placodal development.

To determine if the effects are maintained over a longer period of development, we assayed both the expression of *HuC* and *isl-1* at a slightly later stage, 6 somites, in *dlx3b*-MO- and *dlx4b*-MO-injected embryos (see Fig. 5 about *isl-1* phenotype at 3-somite stage). Consistent with earlier results, we observed a reduction in the number of trigeminal placodal neurons with both *HuC* and *isl-1* (Figs. 3L and N as compared to 3K and M).

dlx3b-MO/dlx4b-MO and EnR-dlx3bhd mRNA act in a dose-dependent manner to position cells at the neural plate border

RB neurons, neural crest and placodes develop within the border between neural and non-neural ectoderm of 3-somite-stage zebrafish neurula. Solomon and Fritz (2002) reported that *dlx3b* and *dlx4b* are required in otic placodal development of the zebrafish. The expression of *pax2a*, a marker of otic placode, is lost in about 11.5 hpf embryos injected with 8 ng *dlx3b*-MO and 8 ng *dlx4b*-MO (Solomon and Fritz, 2002). To examine whether *dlx3b* and *dlx4b* function in the development of RB neurons and trigeminal placodes, expression patterns of marker genes were analyzed in the same concentration (8 ng *dlx3b*-MO and 8 ng *dlx4b*-MO) at 3-somite stage by whole-mount in situ hybridization. *HuC* and *tlx3a* were used to identify RB neurons and trigeminal ganglia (Kim et al., 1996; Langenau et al., 2002). The expression of *HuC* and *tlx3a* were reduced in MO-injected embryos.

The observation that injection of 8 ng *dlx3b*-MO and 8 ng *dlx4b*-MO to embryos caused RB neurons to be reduced lead us to examine the dose-dependency of these morpholinos. *HuC* was chosen as an indicator of the effect in this experiment. In 8 ng *dlx3b*-MO- and 8 ng *dlx4b*-MO-injected embryos, expression of *HuC* marking RB neurons and neurons in trigeminal placodes was reduced (Figs. 4C and D compare with wild type in 4A and B; Table 2). In 16 ng *dlx3b*-MO- and 16 ng *dlx4b*-MO-injected embryos, expression of *HuC* marking RB neurons and neurons in trigeminal placodes was highly reduced or could not be detected (Figs. 4E and F). In addition, some embryos also displayed a slight expanded neural plate in which the expression of *HuC* in those neurons was also highly reduced or absent (not shown). These data show that *HuC* expression in those neurons is sensitive to *dlx3b*-MO and *dlx4b*-MO, and that MOs affect embryos in a dose-dependent fashion. Further, these data suggest that more than 16 ng *dlx3b*-MO and 16 ng *dlx4b*-MO cause RB neurons and placodes to be lost.

In zebrafish, there are 8 *dlx* genes (Panganiban and Rubenstein, 2002). To confirm that *dlx* genes other than *dlx3b* and *dlx4b* do not function before 3-somite stage, 60 or 120 pg *EnR-dlx3bhd* mRNA was injected into the cell of 1-cell-stage embryos, and *HuC* expression was examined at 3-somite stage. The phenotypes of embryos injected with 60 pg *EnR-dlx3bhd* mRNA were similar to those of embryos injected with 8 ng *dlx3b*-MO and 8 ng *dlx4b*-MO. In addition, the phenotypes of embryos injected with 120 pg *EnR-dlx3bhd* mRNA were similar to those of embryos injected with 16 ng *dlx3b*-MO and 16 ng *dlx4b*-MO. In 60 pg *EnR-dlx3bhd* mRNA-injected embryos, the expression of *HuC* marking RB neurons and neurons in trigeminal placodes was reduced (Figs. 4G and H as compared to wild type in 4A and B). In 120 pg *EnR-dlx3bhd* mRNA-injected embryos, the expression of *HuC* was highly

reduced in those neurons (Figs. 4I and J as compared to wild type in 4A and B). The similarity of phenotypes between MO-injected embryos and *EnR-dlx3bhd* mRNA-injected embryos suggests that only *dlx3b* and *dlx4b* function before 3-somite stage in zebrafish.

Effects of the dlx3b/dlx4b MOs on RB neurons and trigeminal placode are specific to these tissues

To confirm that effects of *dlx3b/dlx4b* MOs are specific to the formation of RB neuron and trigeminal placodal development, we examined the expression of other neural markers, *krx20*, *pax2a*, and *axial* as well as mesodermal markers, *gsc*, *ntl*, and *paraxis*, in *dlx3b*-MO- and *dlx4b*-MO-injected embryos. *krx20* is expressed in the hindbrain rhombomeres 3 and 5, while *pax2a* is in the midbrain–hindbrain boundary and the otic placodes (Krauss et al., 1991; Oxtoby and Jowett, 1993). *axial* is expressed within the floor plate of the ventral neural tube and at lower levels in the notochord (Strähle et al., 1993). Analysis of the expression of the neural markers *krx20* and *pax2a* (red), in double in situ hybridization with *HuC* and *isl-1* to detect the RB neuron and TG phenotype (blue), revealed that it was normal in MO-injected embryos (Figs. 5B and D as compared to wild type in 5A and C). The slight broadening of the neural plate was observed by *krx20*, consistent with other findings (noticeable in Fig. 5D). The expression of *axial* (red) in the *dlx3b*-MO- and *dlx4b*-MO-injected embryos was also confirmed to be the same as wild type (Figs. 5F and H as compared to wild type in 5E and G), by double in situ hybridization with *HuC* and *isl-1* to detect the RB neuron and TG phenotype (blue). To determine if mesodermal differentiation was affected in *dlx3b*-MO- and *dlx4b*-MO-injected embryos, we visualized the pattern of expression of *gsc*, *ntl*, and *paraxis*. *gsc* is expressed within the anterior midline, prechordal plate, while *ntl* is primarily expressed within the notochord (Schulte-Merker et al., 1994a,b). *paraxis* has been shown to be expressed strongly in the somitic mesoderm and faintly in the presomitic mesoderm (Shanmugalingam and Wilson, 1998). Consistent with a specific effect of *dlx3b* and *dlx4b* in the specification of RB neurons and trigeminal placodes, no defects on mesodermal marker expression was observed. For *gsc/ntl* (red), we performed double in situ hybridization with *HuC* and *isl-1* to detect the RB neuron and trigeminal placode phenotype (blue; Figs. 5J and L as compared to wild type in 5I and K). For the *paraxis* experiment, we used the same color to detect both *HuC/isl-1* and *paraxis* (blue; arrow to RB neurons), demonstrating that in embryos with reduced expression of RB neurons, no difference was observed in *paraxis* expression (Figs. 5N and P as compared to wild type in Figs. 5M and O).

The concentration of MO injected varies for different genes. Some require on 3–5 ng, while others require much more (Agathon et al., 2001; Busch-Nentwich et al., 2004; Lekven et al., 2001), as is the case for *dlx3b* and *dlx4b*. Because we are injecting a relatively high concentration of MO to see consistent effects on RB neuron and trigeminal placodal development, we wanted to determine if this caused non-specific necrosis of the embryos (reported by Solomon and Fritz, 2002). In *Drosophila*, trypan blue is used to determine the extent of cell death caused by necrosis (Krebs and Feder, 1997). We have determined that this technique is useful in visualizing cell necrosis in zebrafish embryos. For our positive control, we purposely damaged an embryo with a needle, and observed positive trypan blue-stained pattern (Fig. 6D, arrow). However, in the highest doses of *dlx3b* and *dlx4b* MO, or

control MO at the same concentrations, we never observed trypan blue-stained pattern, suggesting that the embryos do not exhibit necrosis at this concentration of MO (Figs. 6B and C as compared to uninjected in 6A or positive control in 6D).

In addition to expression analysis, we designed several experiments to ensure specificity: (1) the injection of *EnR-dlx3bhd* mRNA, (2) the injection of MOs to a different site to block proper splicing of *dlx3b/dlx4b* (E2I2), and (3) the rescue of the MO phenotype with *VP16-dlx3bhd* mRNA. As shown above, the effects of injection of 150 pg *EnR-dlx3bhd* mRNA, examined by the expression of *HuC*, *tlx3a*, and *neuroD*/*pax2a* at 3-somite stage, showed similar phenotypes of embryos injected with *dlx3b*/*dlx4b*-MOs (Figs. 2D, I and 3D, I). These data suggest that the *dlx3b/dlx4b*-MOs are specific to the knockdown of these proteins. In addition, we have further injected E2I2 splice-blocking *dlx3b/dlx4b*-MOs to confirm that MOs made to a different region of the gene will have the same effect, assessed by the expression of the same markers. We have shown definitively that the phenotype of the E2I2 MOs is identical to that of the ATG MOs (Figs. 2 and 3). Finally, we have shown that the overexpression of the *VP16-dlx3bhd* mRNA can rescue the RB neuron phenotype caused by the injection of *dlx3b/dlx4b* MOs (Figs. 6E–I; Table 3). We have used the *VP16-dlx3bhd* mRNA for the rescue, since this construct contains the activating domain VP16 attached to the homeodomain region that is conserved between both genes. These results in combination suggest that the effects of knockdown of *dlx3b* and *dlx4b* are specific to cells at the neural plate border.

dlx3b and dlx4b act upstream of neurogenin1 in trigeminal placode

The *neurogenin* gene family is involved in the specification of sensory neurons, and it is most likely an upstream gene of *neuroD* marking trigeminal placodes in zebrafish (Andermann et al., 2002). In addition, it is also a probable upstream gene of *tlx3a* and *HuC* in RB neuron development (Cornell and Eisen, 2002; Ma et al., 1996). To determine the effects of *dlx3b*-MO and *dlx4b*-MO injection on *neurogenin* expression, we assayed the expression of *neruogenin1* at 3-somite stage. The expression of *neurogenin1* was not changed in the spinal cord of MO-injected embryos at 3-somite stage (Fig. 7B as compared to wild type in 7A). In contrast, the expression of *neurogenin1* in the trigeminal placodes was highly reduced or absent in the placodal primordial region of MO-injected embryos (Fig. 7D as compared to wild type in 7C). These data suggest that *dlx3b* and *dlx4b* begin to function to pattern the neural plate border before 90% epiboly, which is the stage that the expression of *neurogenin1* is first observed.

dlx3b/dlx4b function to regulate the expression of bmp2b at the neural plate border

In chick, based upon expression patterns, it is suggested that there is a regulatory relationship between *DLX5* and *BMP4* (Pera et al., 1999). Similarly, in *Xenopus*, *Xdlx3* regulates *Bmp4* expression at neurula stage (Woda, Kaji and Artinger, in preparation). In zebrafish, *bmp2b* expression was laterally shifted in the non-neural ectoderm of MO-injected embryos at 3-somite stage (not shown). Next, we tested the hypothesis that *bmp2b* expression was altered by injection of *dlx3b* and *dlx4b* MOs at 90% epiboly and at tailbud stage by whole-mount in situ hybridization. *bmp2b* was expressed in the ventral marginal region and the ventral animal region at 90% epiboly and at tailbud stage in wild type

embryos (Fig. 8A). In 90% epiboly wild type embryos, further, *bmp2b* was strongly expressed in a triangular region at the tip of the non-neural ectodermal border (Fig. 8A, arrowhead). In MO-injected embryos, this strong expression was absent and the entire border expression of *bmp2b* was reduced, although expression in the ventral region persisted (Fig. 8B; arrow). In tailbud stage wild–type embryos, *bmp2b* was strongly expressed in the border of the non-neural ectodermal region. In MO-injected embryos, a new region of strong *bmp2b* expression appeared to form, suggesting the formation of a new border region (data not shown). Interestingly, the position of the border in MO-injected embryos was different from that in wild-type embryos.

bmp4 and *bmp7*, as well as *bmp2b*, are also expressed in early stage embryos (Dick et al., 2000; Martínez-Barberá et al., 1997; Nikaido et al., 1997; Schmid et al., 2000). *bmp4* was expressed in the ventral marginal region at 90% epiboly and at tailbud stage in wild-type embryos (Fig. 8C). In MO-injected embryos, the expression pattern of *bmp4* was unchanged (Fig. 8D), although expression was somewhat reduced at tailbud stage (data not shown). *bmp7* was expressed in the ventral marginal region and the ventral animal region at 90% epiboly and at tailbud stage in wild-type embryos (Fig. 8E). In MO-injected embryos, the expression pattern of *bmp7* was not changed at either stage (Fig. 8F). These results suggest that only *bmp2b* expression, and not that of *bmp4* or *bmp7*, is regulated by *dlx3b* and *dlx4b* at 90% epiboly and the relationship is limited to the non-neural ectodermal/neural plate border region.

Differential function of dlx3b and dlx4b in RB neuron and trigeminal placodal development

The above analyses indicate that *dlx3b* and *dlx4b* are required in RB neuron and trigeminal placodal development, but how *dlx3b* and *dlx4b* affect these development is not clear. *dlx3b* and *dlx4b* likely function cell-autonomously in placodal development (Liu et al., 2003; Solomon and Fritz, 2002), but whether this function extends to the other cell type of interest is not known. Here, we have studied how *dlx3b* and *dlx4b* affect both RB neuron and trigeminal placodal development.

In the future lateral region of the trunk in tailbud stage embryos, the expression of *neurogenin1* marks future RB neurons and *dlx3b* expression was adjacent but not overlapping (Figs. 9A–C; arrowheads, *dlx3b* and double arrowhead, *neurogenin1*). This pattern suggests the possibility that *dlx3b* and *dlx4b* act non-cell-autonomously in RB neuron development. To test this hypothesis that *dlx3b* and *dlx4b* act non-cell-autonomously, we created mosaic embryos between wild-type and MO-injected embryos. MO-injected cells were transplanted into wild-type host embryos as well as wild-type cells transplanted into MO-injected embryos at blastula stage. We examined RB neuron and trigeminal placodal development by whole-mount in situ hybridization with the *HuC* probe. In a wild-type background, *HuC*-expressing RB neurons could not be detected in the lateral neural plate when labeled MO-injected cells were situated in the region just outside the neural plate (Figs. 9D–F; rb, RB neurons, mo, MO transplanted cells). In contrast, when labeled wild-type cells expressing normal levels of *dlx3b* and *dlx4b* were transplanted into a MO-injected embryo, *HuC*-expressing RB neurons were seen only around the labeled wild-type transplanted cells (Figs. 9J–L; wt, wild-type transplanted cells). This suggests that a

signal from wild-type cells can rescue locally the effects of the *dlx3b* and *dlx4b* MO. These data demonstrate that *dlx3b* and *dlx4b* function non-cell-autonomously in RB neuron development.

In the future lateral region of the cranial region of tailbud stage embryos, *neurogenin1* is expressed in the future trigeminal placode which overlaps with the expression of *dlx3b* (Figs. 9A–C; double arrow). This pattern suggests the possibility that *dlx3b* and *dlx4b* act cell-autonomously in the development of neurons in trigeminal placodes. To test this hypothesis that *dlx3b* and *dlx4b* act cell-autonomously, mosaic embryos were made and analyzed as in the case of RB neuron development. In a wild-type background, *HuC*-expressing neurons in the trigeminal placode could not be detected there when labeled MO-injected cells occupied the trigeminal placodal region (Figs. 9G–I; tg, neurons in trigeminal placode, mo, MO transplanted cells). In contrast, when labeled wild-type cells expressing normal level of *dlx3b* and *dlx4b* were situated in the trigeminal placodal region of a MO-injected embryo, brown and blue double-labeled neurons in the trigeminal placode were seen (Figs. 9M–O; arrow). These data demonstrate that *dlx3b* and *dlx4b* function cell-autonomously in the development of neurons in the trigeminal placodes. It remains possible that *dlx3b* and *dlx4b* can also act non-cell-autonomously in the trigeminal placode.

Discussion

dlx3b and dlx4b function in RB neuron and trigeminal placodal development in zebrafish

In the present study, using *dlx3b*-MO and *dlx4b*-MO and *EnR-dlx3bhd* mRNA, we have revealed that *dlx3b* and *dlx4b* activities are required for RB neuron and trigeminal placodal development. The expression of genes marking RB neurons and trigeminal placodes were absent, those marking neural crest were slightly reduced, and those marking neural plate were slightly broadened in the embryos injected with MOs or *EnR-dlx3bhd* mRNA (Figs. 2 and 3; and data not shown). In addition, it has been previously reported that *dlx3b* and *dlx4b* act in concert to promote zebrafish otic and olfactory placode formation (Liu et al., 2003; Solomon and Fritz, 2002). This suggests that *dlx3b* and *dlx4b* play multiple roles in the formation of the neural plate border.

How *dlx3b* and *dlx4b* affect the development of RB neurons and trigeminal placodes can be placed in two categories: cell-autonomous and non-cell-autonomous. In the present study, it was revealed that *dlx3b* and *dlx4b* act non-cell-autonomously in RB neuron development and cell-autonomously in trigeminal placodal development. In RB neuron development, *dlx3b*-MO- and *dlx4b*-MO-injected cells in the embryonic epidermis of a wild-type background cannot form *HuC*-positive RB neurons in the lateral neural plate. They prevent their neighbors from becoming the RB neuron fate. In addition, in a MO-injected host background, the transplantation of a single wild-type cell in the embryonic epidermis can rescue the *HuC* expression in RB neurons. This suggests that *dlx3b* and *dlx4b* are sufficient to induce the expression of *HuC* in the lateral neural plate. Since *bmp2b* expression is partially lost in MO-injected embryos, the non-cell-autonomous function of *dlx3b* and *dlx4b* may act via BMP activity. This notion is consistent with many previous reports that BMP actively promotes neural crest and RB neuron development and suppresses neural plate development (Barth et al., 1999; Kishimoto et al., 1997; Nguyen et al., 1998, 2000).

The expression of *neurogenin1*, an upstream gene of *neuroD*, was highly reduced in cranial trigeminal placodes in *dlx3b*-MO- and *dlx4b*-MO-injected embryos. However, the same gene marking RB neurons was normal in the spinal cord region of MO-injected embryos. The expression of *neurogenin1* in the lateral trunk appears at around 90% epiboly (Andermann et al., 2002) in a broad domain at the lateral neural plate. These data in sum suggest the possibility that the non-cell-autonomous function of *dlx3b* and *dlx4b* starts relatively late to affect downstream target genes. Alternatively, if the *dlx3b* and *dlx4b* function commences early, they may affect only gene expression over a very short range. Our preliminary data that the expression of *neuroD* marking RB neurons, which is an immediate downstream gene of *neurogenin1*, was absent in MO-injected embryos would support the latter possibility. *dlx3b* and *dlx4b* also function in a cell-autonomous manner. From the expression of *neurogenin1* in trigeminal placodal region in MO-injected embryos and that of *pax8* in otic placodes in MO-injected embryos (Solomon and Fritz, 2002), it is apparent that this activity begins between 80% and 90% epiboly. In both RB neurons and trigeminal placodes, some common genes are expressed through their development, for example, *neurogenin1*, *neuroD*, *HuC*, and *isl-1*. However, in RB neuron region, the mediolateral reduction of the width of RB neuron region is observed through development, between *neurogenin1* and *neuroD/HuC/isl-1* expression (Blader et al., 1997; Korzh et al., 1998; Ma et al., 1996). The non-cell-autonomous function of *dlx3b* and *dlx4b* may contribute to the event, as well as competitive lateral inhibition by the activities of multiple *delta* genes (Haddon et al., 1998).

The data presented here are consistent with our recent report in *Xenopus* embryos injected with *EnR-Dlx3hd* mRNA, where downstream targets of Dlx proteins were repressed (Woda et al., 2003). However, the neural crest and neural plate phenotypes differ between zebrafish and *Xenopus*. In zebrafish embryos injected with *dlx3b*/*dlx4b*-MO or *EnR-dlx3bhd* mRNA, loss of neural crest did not occur, although a reduction in expression of neural crest marker genes could be seen, and the degree of expansion of neural plate was subtle. In *Xenopus* embryos injected with *EnR-Dlx3hd* mRNA, loss of neural crest is often seen, and the degree of expansion of neural plate is severe (Woda et al., 2003). These data suggest that there is a compensation mechanism in zebrafish that is not present in *Xenopus*. Since *dlx3b*/*dlx4b* and *Xdlx3* are likely to function in a non-cell-autonomous manner for neural crest development in both species, there may be another signal for neural crest development in zebrafish. In fact, in *Xenopus*, *Bmp4* activity is highly reduced in embryos injected with *EnR-Dlx3hd* mRNA (J.W. and K.B.A. unpublished observation). In contrast, in zebrafish, the reduction of *bmp2b* expression was seen only at the non-neural ectodermal border at 90% epiboly, and *bmp4* and *bmp7* expression was almost normal, in MO-injected embryos (Fig. 8). These small reductions of *bmp* genes might also affect the subtleness of phenotype in neural plate of zebrafish (see below).

In the present study, a relatively high concentration of MO is used. As discussed above, *dlx3b* and *dlx4b* may start functioning between 80% and 90% epiboly in the formation of the border between neural and non-neural ectoderm of gastrula and neurula. However, the expression of *dlx3b* begins at a very early embryonic stage, blastula stage, and it is expressed in the entire of epiblast (Fig. 1B; and data not shown). Because of the early-stage

expression of *dlx3b*, the effect of the injected *dlx3b*-MO is reduced at the time when it is required for neural plate border formation (90% epiboly; Fig. 1F). In fact, our analysis of the RT-PCR from cDNA isolated at 2–3-somite-stage wild-type and *dlx3b/dlx4b*-E2I2-MO-injected embryos revealed that by 2–3-somite stage, the reduction in *dlx3b*-E2I2-MO concentration was unable to knockdown dlx3b fully, while the concentration of *dlx4b*-E2I2-MO was sufficient. Gastrulation defects occurred in rare cases in 20 ng *dlx3b*-MO- and 20 ng *dlx4b*-MO-injected embryos, but it did not occur in 40 ng control MO-injected embryos (Table 1). Thus, the early-stage expression of *dlx3b* might contribute to process of epiboly.

Two different *dlx3b/dlx4b*-MOs were used to study the function of these genes. One is *dlx3b/dlx4b* ATG MO, which binds to the translation initiation site of the mRNA, and the other is *dlx3b/dlx4b* E2I2 MO, which bind the exon2–intron2 boundary of their nuclear RNA. Phenotypes in RB neurons and trigeminal placodes by *dlx3b/dlx4b* E2I2 MO were slightly milder than those by *dlx3b/dlx4b* ATG MO. It is known that some *Dlx* genes, for example mouse *Dlx5* and *Dlx4*, produce multiple transcripts by alternative splicing (Liu et al., 1997; Nakamura et al., 1996; Yang et al., 1998). From the difference of the degree in phenotypes, there is a possibility of the existence of alternatively spliced forms of *dlx3b*. In addition, we observed a wild-type form present after the E2I2–*dlx3b*-MO injection, which could compensate for the function of the alternate spliced form at later stages (2–3-somite stage). However, since the phenotype is consistent with the ATG-MOs and EnR–dlx3bhd, we believe that there is sufficient knockdown of the dlx3b at the appropriate time (90% epiboly) to produce specific phenotypes.

dlx3b and dlx4b may intensify bmp2b activity at the non-neural ectodermal border of gastrula in zebrafish

In zebrafish and *Xenopus*, the BMP activity gradient model is widely supported as a mechanism of neural crest formation (Aybar and Mayor, 2002; Nguyen et al., 1998, 2000). A BMP activity gradient in the ectoderm of the gastrula stage is established by an interaction between BMPs produced in the ectoderm and BMP inhibitors secreted from the dorsal mesoderm. In the ectoderm, high levels of BMP activity specify the epidermis, and low levels specify the neural plate. Intermediate levels specify the fate of cells at the neural plate border. Our data reveal that there is a region of strong *bmp2b* expression, at the border of non-neural and neural ectoderm at 90% epiboly, and that this expression of *bmp2b* is lost in *dlx3b*-MO- and *dlx4b*-MO-injected embryos. This result suggests that the specification of cells at the neural plate border in zebrafish may be more complex than simply relying on the BMP activity gradient alone. BMP activity at the border may be slightly higher than is currently suggested. In fact, the neural crest region did not expand laterally and its marker gene expression was slightly reduced in MO-injected embryos, where subtle loss of *bmp2b* expression is seen. The phenotype is much different from *somitabun* and *snailhouse* mutant embryos, which also have low levels of BMP activity and show the phenotype of the expanded neural crest region (Nguyen et al., 1998). *dlx3b* and *dlx4b* may function in intensifying BMP activity at the border region, rather than keeping the simple gradient of BMP activity in the ectoderm. The difference of the degree of phenotypes between RB neurons and neural crest in MO-injected embryos may be explained by the fact that RB neuron development is more sensitive to the optimal level of BMP activity than neural crest

cells. We did not study the function of *dlx3b* before 80% epiboly, when the broad homogeneous expression of *dlx3b* overlaps with *bmp2b* on the ventral side of the gastrula. Thus, we cannot rule out the possibility that *dlx3b* regulates *bmp2b* gene expression during early gastrulation. If there is a role for *dlx3b* earlier than 80% epiboly, *dlx3b* function may be separated into two phases: (1) keeping BMP activity in the non-neural ectoderm before 80% epiboly, and (2) intensifying BMP activity in the non-neural ectodermal border at 90% epiboly. This is an interesting issue that remains to be studied in detail.

The loss of the strong *bmp2b*-expressing triangle region at the tip of the non-neural ectodermal border resulted in a curved *bmp2b*-expressing non-neural ectodermal region (Fig. 8). In the ectoderm of the gastrula, the *bmp2b*-expressing region and the neural ectodermal region are always complementary (Muraoka et al., 2000; Nikaido et al., 1999). The loss of *bmp2b* expression may be involved in the expansion of the neural plate in MO-injected embryos. Interestingly, a new region of intense *bmp2b* expression appears as a presumably new non-neural ectodermal border forms. This occurs at tailbud stage in the MO-injected embryos (data not shown), and the expression persists at least to 3-somite stage. It appears at a different position, and thus it is clear that it is a different border from the original wild-type border. This suggests that *dlx3b* and *dlx4b* may play a role in defining the shape of the non-neural ectodermal border at 90% epiboly.

Acknowledgments

The authors thank Dr. G. Boekhoff-Falk (Panganiban) and Dr. J. Kohtz and Dr. J. Feng for the Dll antibody, Dr. M.C. Mullins and Dr. M. Hammerschmidt for providing *bmp7*, Dr. M. Ekker for *dlx4b*, Dr. S. Wilson for *paraxis*, and others. We would also like to thank Dr. David Stock for providing *dlx3b/dlx4b* genomic sequence and for discussions; Dr. Linda Barlow for critical reading of the manuscript; Laura Hernandez and Dawn Riedel for excellent technical assistance and Pete Simpson for technical assistance and fish care/maintenance. We gratefully acknowledge the support of NIH/NIDCR (K22DE14200) to KBA.

References

Agathon A, Thisse B, Thisse C. Morpholino knock-down of antivin1 and antivin2 upregulates nodal signaling. Genesis. 2001; 30:178–182. [PubMed: 11477702]

Andermann P, Ungos J, Raible DW. Neurogenin1 defines zebrafish cranial sensory ganglia precursors. Dev. Biol. 2002; 251:45–58. [PubMed: 12413897]

Appel B, Korzh V, Glasgow E, Thor S, Edlund T, Dawid IB, Eisen JS. Motoneuron fate specification revealed by patterned LIM homeobox gene expression in embryonic zebrafish. Development. 1995; 121:4117–4125. [PubMed: 8575312]

Artinger KB, Chitnis AB, Mercola M, Driever W. Zebrafish *narrowminded* suggests a genetic link between formation of neural crest and primary sensory neurons. Development. 1999; 126:3969–3979. [PubMed: 10457007]

Aybar MJ, Mayor R. Early induction of neural crest cells: lessons learned from frog, fish and chick. Curr. Opin. Genet. Dev. 2002; 12:452–458. [PubMed: 12100892]

Baker CVH, Bronner-Fraser M. Vertebrate cranial placodes. I. Embryonic induction. Dev. Biol. 2001; 232:1–61. [PubMed: 11254347]

Bally-Cuif L, Hammerschmidt M. Induction and patterning of neuronal development, and its connection to cell cycle control. Curr. Opin. Neurobiol. 2003; 13:16–25. [PubMed: 12593978]

Barth KA, Kishimoto Y, Rohr KB, Seydler C, Schulte-Merker S, Wilson SW. Bmp activity establishes a gradient of positional information throughout the entire neural plate. Development. 1999; 126:4977–4987. [PubMed: 10529416]

Blader P, Fischer N, Gradwohl G, Guillemot F, Strähle U. The activity of Neurogenin1 is controlled by local cues in the zebrafish embryo. Development. 1997; 124:4557–4569. [PubMed: 9409673]

Busch-Nentwich E, Sollner C, Roehl H, Nicolson T. The deafness gene *dfna5* is crucial for *ugdh* expression and HA production in the developing ear in zebrafish. Development. 2004; 131:943–951. [PubMed: 14736743]

Cornell RA, Eisen JS. Delta/Notch signaling promotes formation of zebrafish neural crest by repressing Neurogenin1 function. Development. 2002; 129:2639–2648. [PubMed: 12015292]

Dick A, Hild M, Bauer H, Imai Y, Maifeld H, Schier AF, Talbot WS, Bouwmeester T, Hammerschmidt M. Essential role of Bmp7 (*snailhouse*) and its prodomain in dorsoventral patterning of the zebrafish embryo. Development. 2000; 127:343–354. [PubMed: 10603351]

Draper BW, Morcos PA, Kimmel CB. Inhibition of zebrafish *fgf8* pre-mRNA splicing with morpholino oligos: a quantifiable method for gene knockdown. Genesis. 2001; 30:154–156. [PubMed: 11477696]

Ekker M, Akimenko MA, Bremiller R, Westerfield M. Regional expression of three homeobox transcripts in the inner ear of zebrafish embryos. Neuron. 1992; 9:27–35. [PubMed: 1352984]

Feledy JA, Beanan MJ, Sandoval JJ, Goodrich JS, Lim JH, Matsuo-Takasaki M, Sato SM, Sargent TD. Inhibitory patterning of the anterior neural plate in *Xenopus* by homeodomain factors *Dlx3* and *Msx1*. Dev. Biol. 1999; 212:455–464. [PubMed: 10433834]

Haddon C, Smithers L, Schneider-Maunoury S, Coche T, Henrique D, Lewis J. Multiple *delta* genes and lateral inhibition in zebrafish primary neurogenesis. Development. 1998; 125:359–370. [PubMed: 9425132]

Kim C, Ueshima E, Muraoka O, Tanaka H, Yeo S, Huh T, Miki N. Zebrafish *elav*/HuC homologue as a very early neuronal marker. Neuro. Lett. 1996; 216:109–112.

Kishimoto Y, Lee K, Zon L, Hammerschmidt M, Schulte-Merker S. The molecular nature of zebrafish *swirl*: BMP2 function is essential during early dorsoventral patterning. Development. 1997; 124:4457–4466. [PubMed: 9409664]

Korzh V, Edlund T, Thor S. Zebrafish primary neurons initiate expression of the LIM homeodomain protein Isl-1 at the end of gastrulation. Development. 1993; 118:417–425. [PubMed: 8223269]

Korzh V, Sleptsova I, Liao J, He J, Gong Z. Expression of zebrafish bHLH genes *ngn1* and *nrd* defines distinct stages of neural differentiation. Dev. Dyn. 1998; 213:92–104. [PubMed: 9733104]

Krauss S, Johansen T, Korzh V, Fjose A. Expression of the zebrafish paired box gene *pax[zf-b]* during early neurogenesis. Development. 1991; 113:1193–1206. [PubMed: 1811936]

Krebs RA, Feder ME. Tissue-specific variation in Hsp70 expression and thermal damage in *Drosophila melanogaster* larvae. J. Exp. Biol. 1997; 200:2007–2015. [PubMed: 9246784]

Langenau DM, Palomero T, Kanki JP, Ferrando AA, Zhou Y, Zon LI, Look AT. Molecular cloning and developmental expression of *Tlx (Hox11)* genes in zebrafish (*Danio rerio*). Mech. Dev. 2002; 117:243–248. [PubMed: 12204264]

Lekven AC, Thorpe CJ, Waxman JS, Moon RT. Zebrafish *wnt8* encodes two *wnt8* proteins on a bicistronic transcript and is required for mesoderm and neurectoderm patterning. Dev. Cell. 2001; 1:103–114. [PubMed: 11703928]

Liu JK, Ghattas I, Liu S, Chen S, Rubenstein JLR. Dlx genes encode DNA-binding proteins that are expressed in an overlapping and sequential pattern during basal ganglia differentiation. Dev. Dyn. 1997; 210:498–512. [PubMed: 9415433]

Liu D, Chu H, Maves L, Yan Y, Morcos PA, Postlethwait JH, Westerfield M. Fgf3 and Fgf8 dependent and independent transcription factors are required for otic placode specification. Development. 2003; 130:2213–2224. [PubMed: 12668634]

Ma Q, Kintner C, Anderson DJ. Identification of *neurogenin*, a vertebrate neuronal determination gene. Cell. 1996; 87:43–52. [PubMed: 8858147]

Martínez-Barberá JP, Toresson H, Da Rocha S, Krauss S. Cloning and expression of three members of the zebrafish Bmp family: *Bmp2a*, *Bmp2b* and *Bmp4*. Gene. 1997; 198:53–59. [PubMed: 9370264]

McLarren KW, Litsiou A, Streit A. DLX5 positions the neural crest and preplacode region at the border of the neural plate. Dev. Biol. 2003; 259:34–47. [PubMed: 12812786]

Muraoka O, Ichikawa H, Shi H, Okumura S, Taira E, Higuchi H, Hirano T, Hibi M, Miki N. Kheper, a novel ZFH/δEF1 family member, regulates the development of the neuroectoderm of zebrafish (*Danio rerio*). Dev. Biol. 2000; 228:29–40. [PubMed: 11087624]

Nakamura S, Stock DW, Wydner KL, Bollekens JA, Takeshita K, Nagai BM, Chiba S, Kitamura T, Freeland TM, Zhao Z, Minowada J, Lawrence JB, Weiss KM, Ruddle FH. Genomic analysis of a new mammalian Distal-less gene: Dlx7. Genomics. 1996; 38:314–324. [PubMed: 8975708]

Nasevicius A, Ekker SC. Effective targeted gene 'knockdown' in zebrafish. Nat. Genet. 2000; 26:216–220. [PubMed: 11017081]

Nguyen VH, Schmid B, Trout J, Connors SA, Ekker M, Mullins MC. Ventral and lateral regions of the zebrafish gastrula, including the neural crest progenitors, are established by a *bmp2b/swirl* pathway of genes. Dev. Biol. 1998; 199:93–110. [PubMed: 9676195]

Nguyen VH, Trout J, Connors SA, Andermann P, Weinberg E, Mullins MC. Dorsal and intermediate neuronal cell types of the spinal cord are established by a BMP signaling pathway. Development. 2000; 127:1209–1220. [PubMed: 10683174]

Nikaido M, Tada M, Saji Y, Ueno N. Conservation of BMP signaling in zebrafish mesoderm patterning. Mech. Dev. 1997; 61:75–88. [PubMed: 9076679]

Nikaido M, Tada M, Takeda H, Kuroiwa A, Ueno N. In vivo analysis using variants of zebrafish BMPR-IA: range of action and involvement of BMP in ectoderm patterning. Development. 1999; 126:181–190. [PubMed: 9834197]

Odenthal J, Nqsslein-Volhard C. *Fork head* domain genes in zebrafish. Dev. Genes Evol. 1998; 208:245–258. [PubMed: 9683740]

Oxtoby E, Jowett T. Cloning of the zebrafish *krox-20* gene (*krx-20*) and its expression during hindbrain development. Nuc. Acid. Res. 1993; 21:1087–1095.

Panganiban G, Rubenstein JLR. Developmental functions of the *Distal-less*/Dlx homeobox genes. Development. 2002; 129:4371–4386. [PubMed: 12223397]

Panganiban G, Sebring A, Nagy L, Carroll S. The development of crustacean limbs and the evolution of arthropods. Science. 1995; 270:1363–1366. [PubMed: 7481825]

Pera E, Stein S, Kessel M. Ectodermal patterning in the avian embryo: epidermis versus neural plate. Development. 1999; 126:63–73. [PubMed: 9834186]

Sawada A, Fritz A, Jiang Y, Yamamoto A, Yamasu K, Kuroiwa A, Saga Y, Takeda H. Zebrafish *Mesp* family genes, *mesp-a* and *mesp-b* are segmentally expressed in the presomitic mesoderm, and *Mesp*-b confers the anterior identity to the developing somite. Development. 2000; 127:1691–1702. [PubMed: 10725245]

Schier AF, Neuhauss SCF, Helde KA, Talbot WS, Driever W. The *one-eyed pinhead* gene functions in mesoderm and endoderm formation in zebrafish and interacts with *no tail*. Development. 1997; 124:327–342. [PubMed: 9053309]

Schlosser G, Northcutt RG. Development of neurogenic placodes in *Xenopus laevis*. J. Comp. Neurol. 2000; 418:121–146. [PubMed: 10701439]

Schmid B, Fürthauer M, Connors SA, Trout J, Thisse B, Thisse C, Mullins MC. Equivalent genetic roles for *bmp7/snailhouse* and *bmp2b/swirl* in dorsoventral pattern formation. Development. 2000; 127:957–967. [PubMed: 10662635]

Schulte-Merker S, Hammerschmidt M, Beuchle D, Cho KW, De Robertis EM, Nqsslein-Volhard C. Expression of zebrafish *goosecoid* and *no tail* gene products in wild-type and mutant *no tail* embryos. Development. 1994; 120:843–852. [PubMed: 7600961]

Schulte-Merker S, van Eeden FJM, Halpern ME, Kimmel CB, Nqsslein-Volhard C. *No tail (ntl)* is the zebrafish homologue of the mouse *T* (*Brachyury*) gene. Development. 1994; 120:1009–1015. [PubMed: 7600949]

Shanmugalingam S, Wilson SW. Isolation, expression and regulation of a zebrafish *paraxis* homologue. Mech. Dev. 1998; 78:85–89. [PubMed: 9858695]

Solnica-Krezel L, Driever W. Microtubule arrays of the zebrafish yolk cell: organization and function during epiboly. Development. 1994; 120:2443–2455. [PubMed: 7956824]

Solomon KS, Fritz A. Concerted action of two *dlx* paralogs in sensory placode formation. Development. 2002; 129:3127–3136. [PubMed: 12070088]

Strähle U, Blader P, Henrique D, Ingham PW. Axial, a zebrafish gene expressed along the developing body axis, shows altered expression in cyclops mutant embryos. Genes Dev. 1993; 7:1436–1446. [PubMed: 7687227]

Thisse C, Thisse B. High resolution whole-mount in situ hybridization. Zebra. Scien. Monit. 1998; 15:8–9.

Torres M, Gómez-Pardo E, Gruss P. *Pax2* contributes to inner ear patterning and optic nerve trajectory. Development. 1996; 122:3381–3391. [PubMed: 8951055]

Westerfield, M. THE ZEBRAFISH BOOK. Eugene: The University of Oregon Press; 1993.

Woda JM, Pastagia J, Mercola M, Artinger KB. Dlx proteins position the neural plate border and determine adjacent cell fates. Development. 2003; 130:331–342. [PubMed: 12466200]

Yang L, Zhang H, Hu G, Wang H, Abate-Shen C, Shen MM. An early phase of embryonic *Dlx5* expression defines the rostral boundary of the neural plate. J. Neurosci. 1998; 18:8322–8330. [PubMed: 9763476]

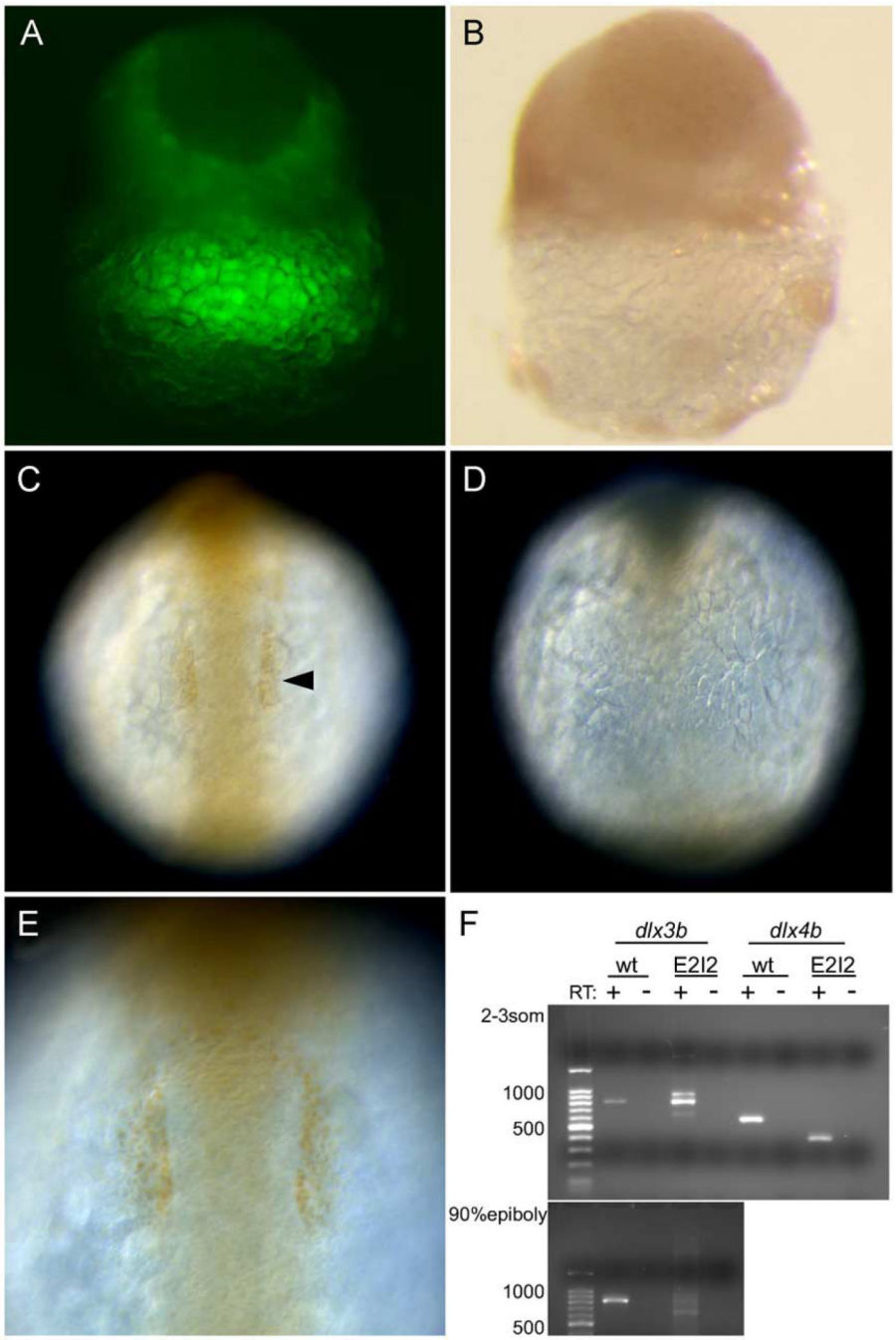

Fig. 1.

Knockdown of dlx proteins in embryos injected with *dlx3b/dlx4b*-ATG-MOs and *dlx3b/dlx4b*-E2I2-MOs. The knockdown by the ATG-MOs was revealed by immunostaining with anti-Dll antibody (A–E). (A and B) Late blastula embryos. (C–E) 6-somite-stage embryos. (C and E) Wild-type embryos. (A, B, D) ATG-MO-injected embryos. (A and B) Same images of a blastula. (A) Fluorescence image revealing MOs + LFD, and (B) bright field. The dispersion of MOs and anti-Dll immunoreactivity are complementary in the epiblast. Lateral views. (C and D) Anti-Dll antibody immunoreactivity in the otic placodal

primordium (arrowhead) is absent in MO-injected embryos. Dorsal views, anterior is to the top. (E) The magnification view of the otic placodal primordium in (C). The knockdown by the E2I2-MOs was revealed by RT-PCR followed by gel electrophoresis (F). (F) Wild type (wt) as compared to E2I2 MO (E2I2) *dlx3b* and *dlx4b* RT-PCR products. In *dlx3b* RT-PCR, at 2–3-somite stage, the amplification of cDNA from wild-type embryos produced an 810-bp band, and cDNA from E2I2-MO-injected embryos produced three bands of 630, 810, and 900 -bp in size. At 90% epiboly, in E2I2-MO-injected embryos, the 810-bp band was faint. In *dlx4b* RT-PCR, at 2- to 3-somite stage, the amplification of cDNA from wild-type embryos produced a 580-bp band, and cDNA from E2I2-MO-injected embryos produced a 390-bp band. Negative-control reactions run in parallel, where reverse transcriptase was omitted in the cDNA synthesis reactions (RT−).

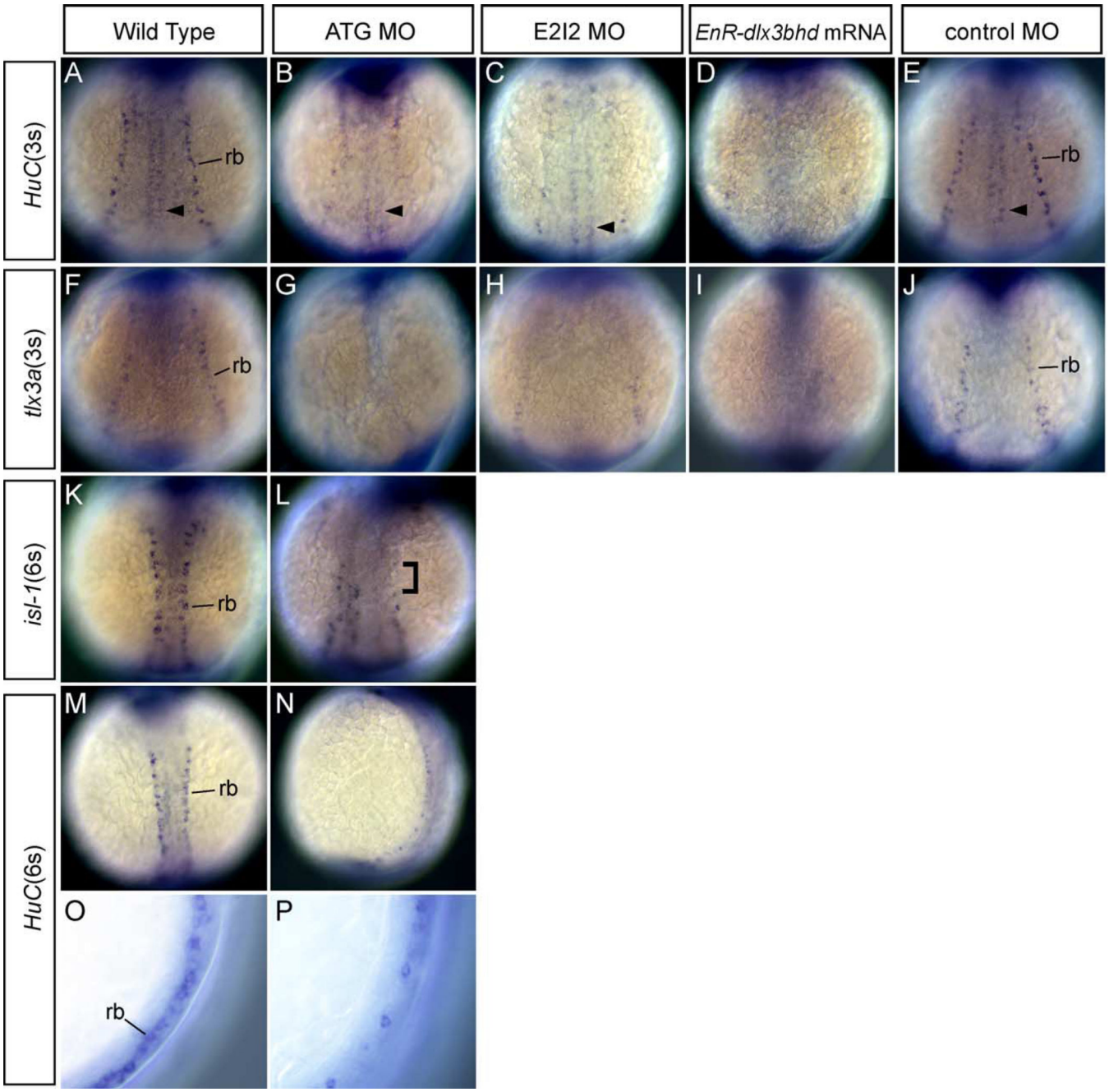

Fig. 2.

Phenotypes of Rohon-Beard (RB) sensory neurons in MOs and *EnR-dlx3bhd* mRNA injected embryos at 3- and 6-somite stage. (A–J) Embryos at 3-somite stage. Dorsal views, anterior is to the top. (K–P) Embryos at 6-somite stage. (A, F, K, M, O) Wild-type embryos. (B, G, L, N, P) 20 ng ATG-*dlx3b*-MO/20 ng ATG-*dlx4b*-MO-injected embryos. (C and H) 20 ng E2I2-*dlx3b*-MO/20 ng E2I2-*dlx4b*-MO-injected embryos. (D and I) One hundred fifty-picogram *EnR-dlx3bhd* mRNA-injected embryos. (E and J) Forty-nanogram control MO-injected embryos. (A–E, M–P) Expression of *HuC*. (F–J) Expression of *tlx3a*. (K and L) Expression of *isl-1*. (O) High magnification lateral view of a wild-type embryo. (P) High

magnification lateral view of (N). In (A), RB neurons (rb) and primary motor neurons (arrowhead) are seen. After injection of *dlx3b* and *dlx4b*-MOs or *EnR-dlx3bhd* mRNA (B–D), primary motor neurons are present, but RB neurons are highly reduced or absent, as seen by the expression of *HuC*. A control MO injected at the same concentration in (E) has normal RB neurons. In (G–I), RB neurons are highly reduced or absent after injection of *dlx3b* and *dlx4b*-MOs or *EnR-dlx3bhd* mRNA, observed with *tlx3a* expression. In a control MO injected at the same concentration in (J), no changes are observed. In embryos allowed to develop until the 6-somite stage (L and N), RB neurons continue to show a reduction after injection of *dlx3b* and *dlx4b*-MOs. The bracket in (L) shows the region of no RB neurons. In a higher magnification view (O and P), it is easily recognized that RB neurons are highly reduced in MO-injected embryos observed at 6-somite stage.

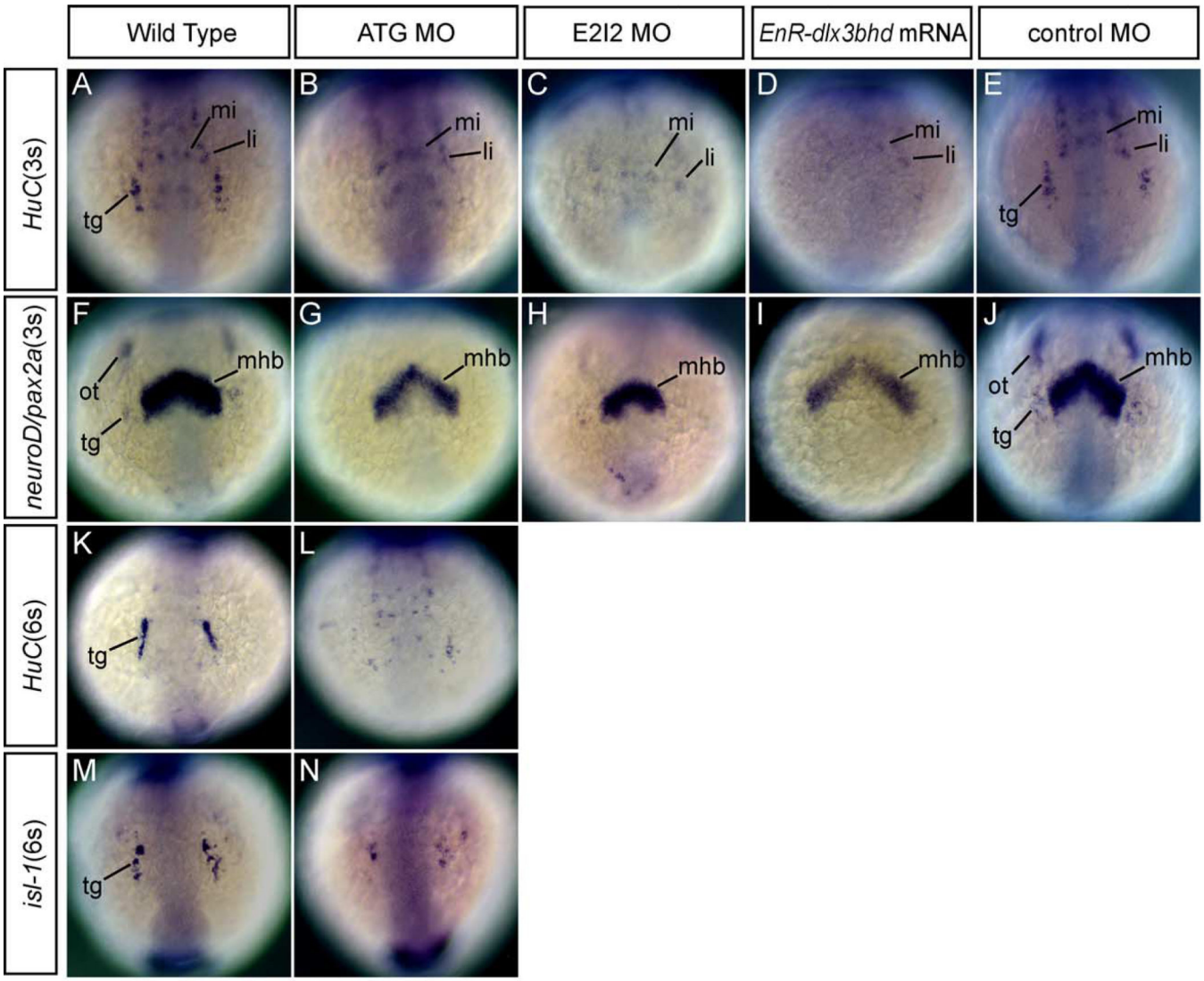

Fig. 3.

Phenotypes of neurons in the trigeminal placodes in MOs and *EnR-dlx3bhd* mRNA injected embryos at 3- and 6-somite stage. (A–J) Embryos at 3-somite stage. Anterior views. (K–N) Embryos at 6-somite stage. Anterior views. (A, F, K, M) Wild-type embryos. (B, G, L, N) 20 ng ATG-*dlx3b*-MO/20 ng ATG-*dlx4b*-MO-injected embryos. (C and H) 20 ng E2I2-*dlx3b*-MO/20 ng E2I2-*dlx4b*-MO-injected embryos. (D and I) One hundred fifty-picogram *EnR-dlx3bhd* mRNA-injected embryos. (E and J) Forty-nanogram control MO-injected embryos. (A–E, K, L) Expression of *HuC*. (F–J) Expression of *neuroD/pax2a*. (M and N) Expression of *isl-1*. In a wild-type embryo (A), neurons in the trigeminal placodes (tg) and anterior lateral/medial hindbrain interneurons (li, mi) are observed. After injection of *dlx3b* and *dlx4b*-MOs or *EnR-dlx3bhd* mRNA shown in (B–D), anterior lateral/medial hindbrain interneurons remain, but neurons in the trigeminal placodes are highly reduced or absent as shown by expression of *HuC*. In a control-MO injected embryo (E), neurons in the trigeminal placodes are seen in the placodal primordial region. *neuroD/pax2a* expression in (G–I), both are highly reduced or absent in the placodal primordial region following

injection of *dlx3b* and *dlx4b*-MOs or *EnR-dlx3bhd* mRNA. Midbrain–hindbrain boundary is seen in the central nervous system (mhb). In a control MO-injected embryos (J), no changes were observed in the trigeminal (tg) and otic placodal primordia (ot). Shown at the 6-somite stage, expression of *HuC* (L) and *isl-1* (N), neurons in the trigeminal placodes remain highly reduced, as compared to wild-type embryos in (K and M), respectively.

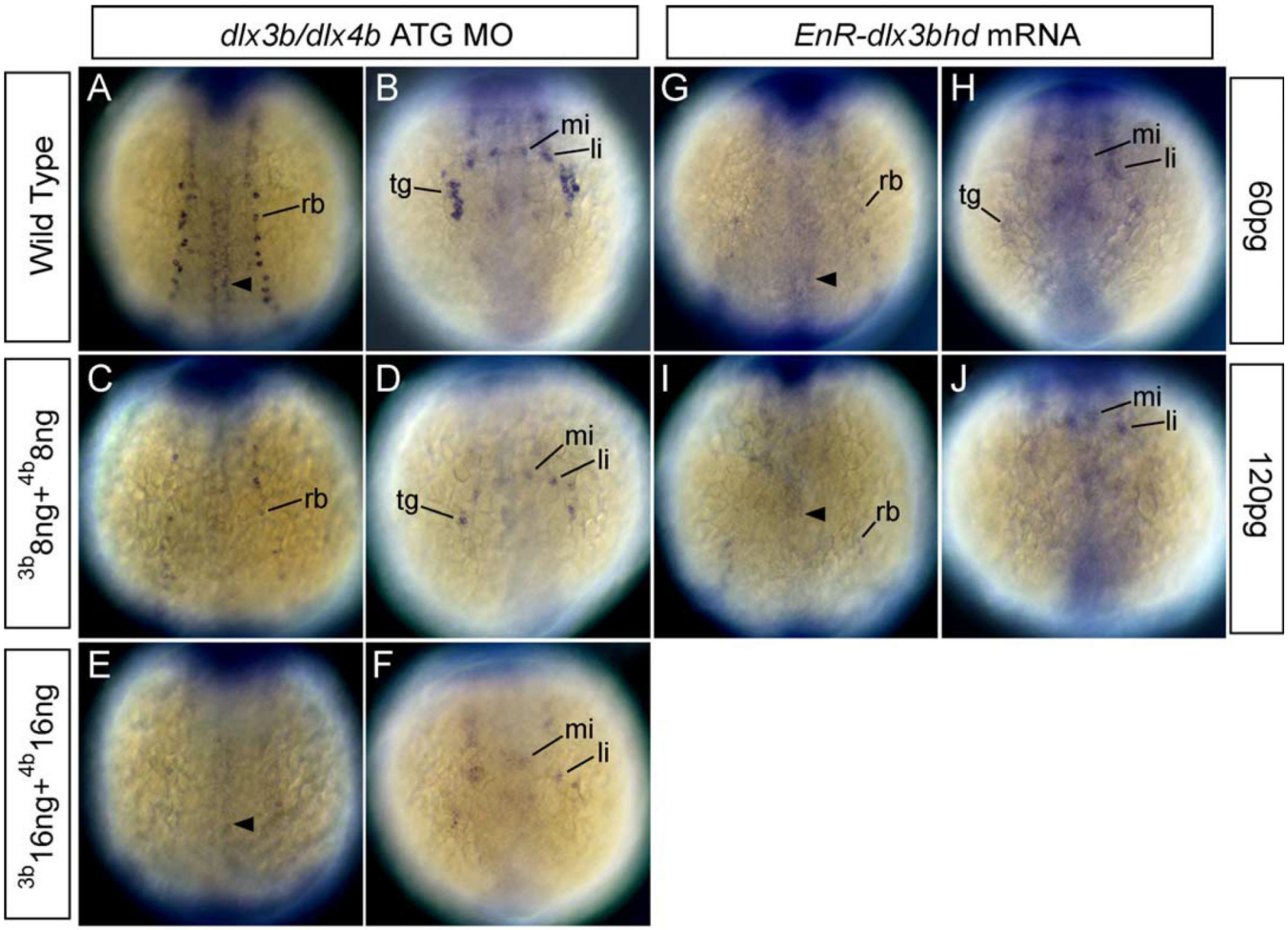

Fig. 4.

HuC expression in embryos injected with *dlx3b*-ATG-MO and *dlx4b*-ATG-MO and *EnR-dlx3bhd* mRNA at 3-somite stage. (A, C, E, G, I) Dorsal views, anterior is to the top. (B, D, F, H, J) Anterior views. (A and B) Wild-type embryos. (C and D) 8 ng *dlx3b*-MO- and 8 ng *dlx4b*-MO-injected embryos. (E and F) 16 ng *dlx3b*-MO- and 16 ng *dlx4b*-MO-injected embryos. (G and H) 60 pg *EnR-dlx3bhd* mRNA-injected embryos. (I and J) 120 pg *EnR-dlx3bhd* mRNA-injected embryos. (A–F) and (G–J) show that the expression of *HuC*, which is expressed in RB neurons in the trunk (rb) and neurons in trigeminal placodes in the head (tg), is gradually reduced as the concentration of MOs and *EnR-dlx3bhd* mRNA are increased. In contrast, primary motor neurons (arrowhead) and anterior lateral hindbrain interneurons (li) and anterior medial hindbrain interneurons (mi) are not changed.

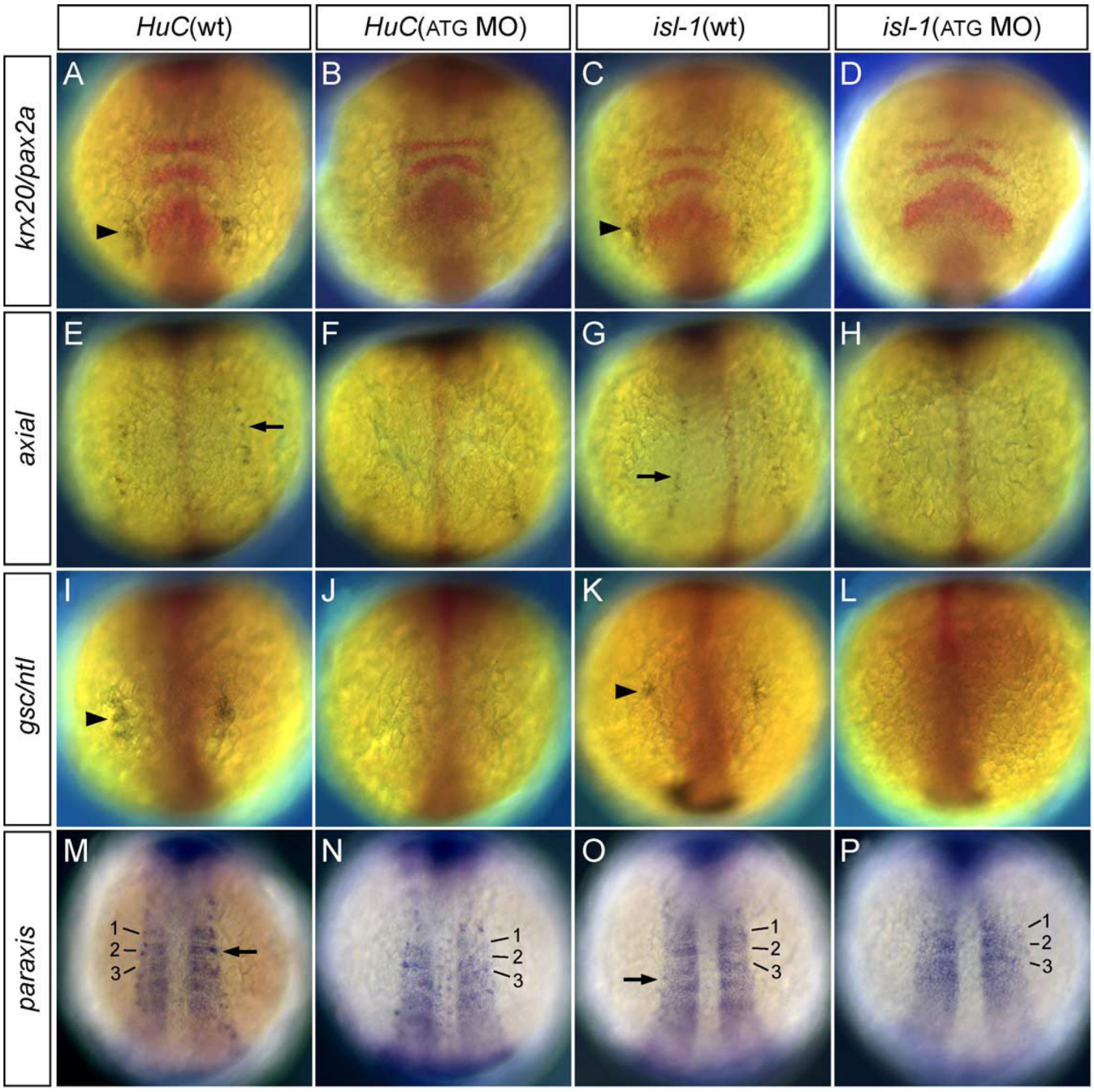

Fig. 5.

Double in situ hybridization of *HuC/isl-1* and neural/mesodermal markers in MO-injected embryos. (A, C, E, G, I, K, M, O) Wild-type embryos at 3-somite stage. (B, D, F, H, J, L, N, P) 20 ng ATG-*dlx3b*-MO/20 ng ATG-*dlx4b*-MO-injected embryos at 3-somite stage. (A and B) Expression of *HuC* (blue) and *krx20/pax2a*, a marker of rhombomeres 3 and 5 and midbrain–hindbrain boundary (red). (C and D) Expression of *isl-1* (blue) and *krx20/pax2a* (red). (E and F) Expression of *HuC* (blue) and *axial* marking floor plate (red). (G and H) Expression of *isl-1* (blue) and *axial* (red). (I and J) Expression of *HuC* (blue) and *gsc/ntl*

expressed in the prechordal plate and notochord (red). (K and L) Expression of *isl-1* (blue) and *gsc/ntl* (red). (M and N) Expression of *HuC* (blue) and *paraxis* showing expression in the somites (blue). Numbers 1–3 correspond to the somites. (O and P) Expression of *isl-1* (blue) and *paraxis* (blue). Numbers 1– 3 correspond to the somites. In (B, D, J, L), neurons in the trigeminal placodes (arrowhead) are highly reduced or absent, shown by the expression of *HuC* and *isl-1*. The expression of *HuC* and *isl-1* in the RB neurons (F, H, N, P; arrow) are highly reduced or absent. However, no changes are observed in neural/mesodermal marker expression in *dlx3b* and *dlx4b* MO-injected embryos (B, D, F, H, J, L, N, P).

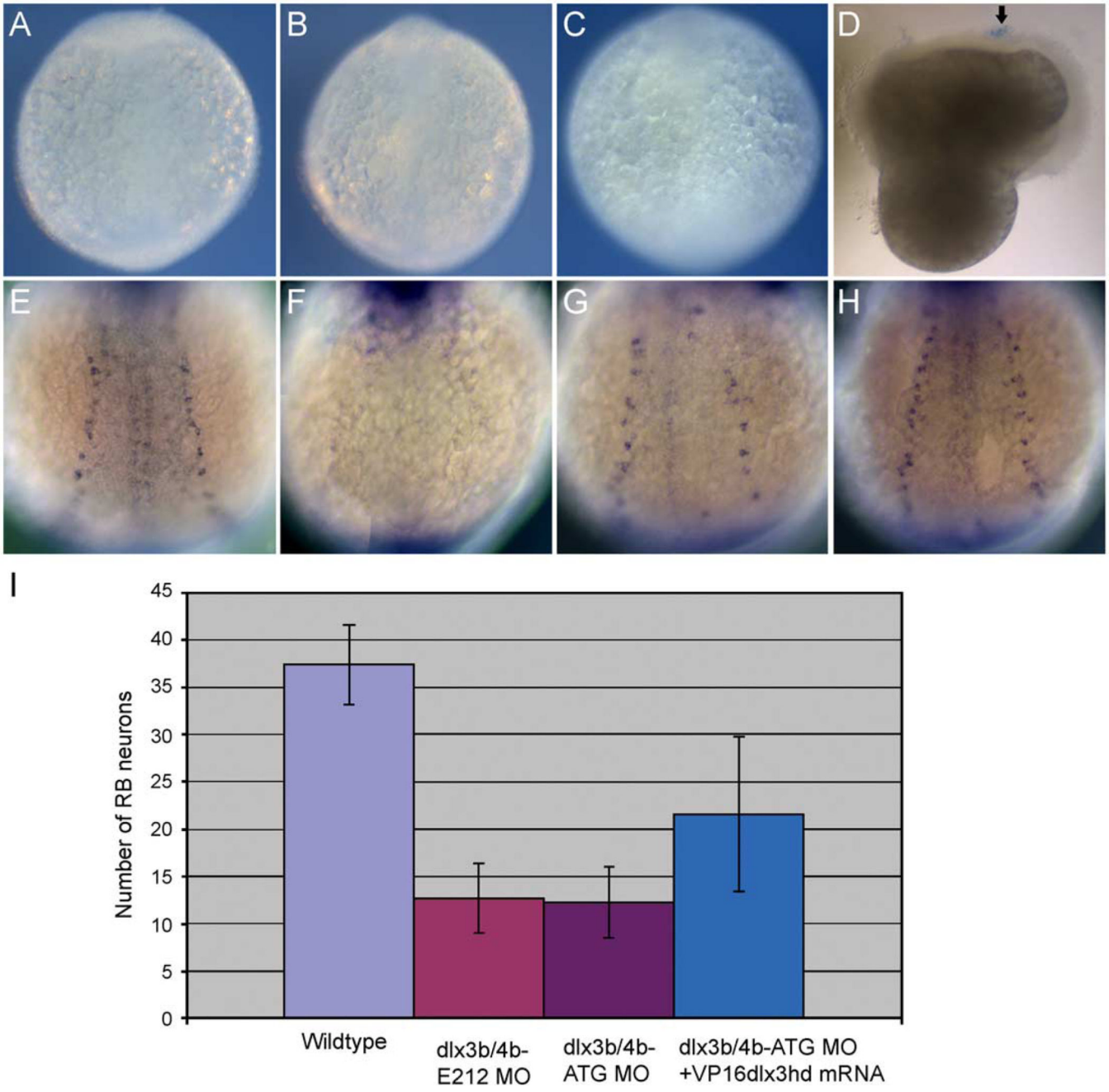

Fig. 6.

Study of necrosis and rescued phenotypes of RB neurons by *VP16-dlx3bhd* mRNA in *dlx3b* and *dlx4b* MO-injected embryos. Trypan blue-stained pattern in 2–3-somite-stage embryos (A–D) and *HuC*-expressing RB neuron pattern in 3-somite-stage embryos (E–H). (A) A wild-type embryo. (B) A 20-ng ATG-*dlx3b*-MO/20 ng ATG-*dlx4b*-MO-injected embryo. (C) A 40-ng control MO-injected embryo. (D) An embryo injured by a tungsten needle. No trypan blue-stained pattern is seen in wild type, 20 ng ATG-*dlx3b*-MO/20 ng ATG-*dlx4b*-MO-injected, and 40 ng control MO-injected embryos (A–C). In the injured embryo (D), a blue-stained pattern can be seen (arrow), indicating cell necrosis. (E) A wild-type embryo

expressing *HuC*. (F) An embryo injected with 20 ng ATG-*dlx3b*-MO/20 ng ATG-*dlx4b*-MO. (G) A partially rescued embryo in RB neurons by *VP16-dlx3bhd* mRNA, injected with 20 ng ATG-*dlx3b*-MO/20 ng ATG-*dlx4b*-MO. (H) A fully rescued embryo in RB neurons by *VP16-dlx3bhd* mRNA, injected with 20 ng ATG-*dlx3b*-MO/20 ng ATG-*dlx4b*-MO. (I) Numbers of RB neurons are recovered in MO-injected embryos by injection of 150 pg *VP16-dlx3bhd* mRNA.

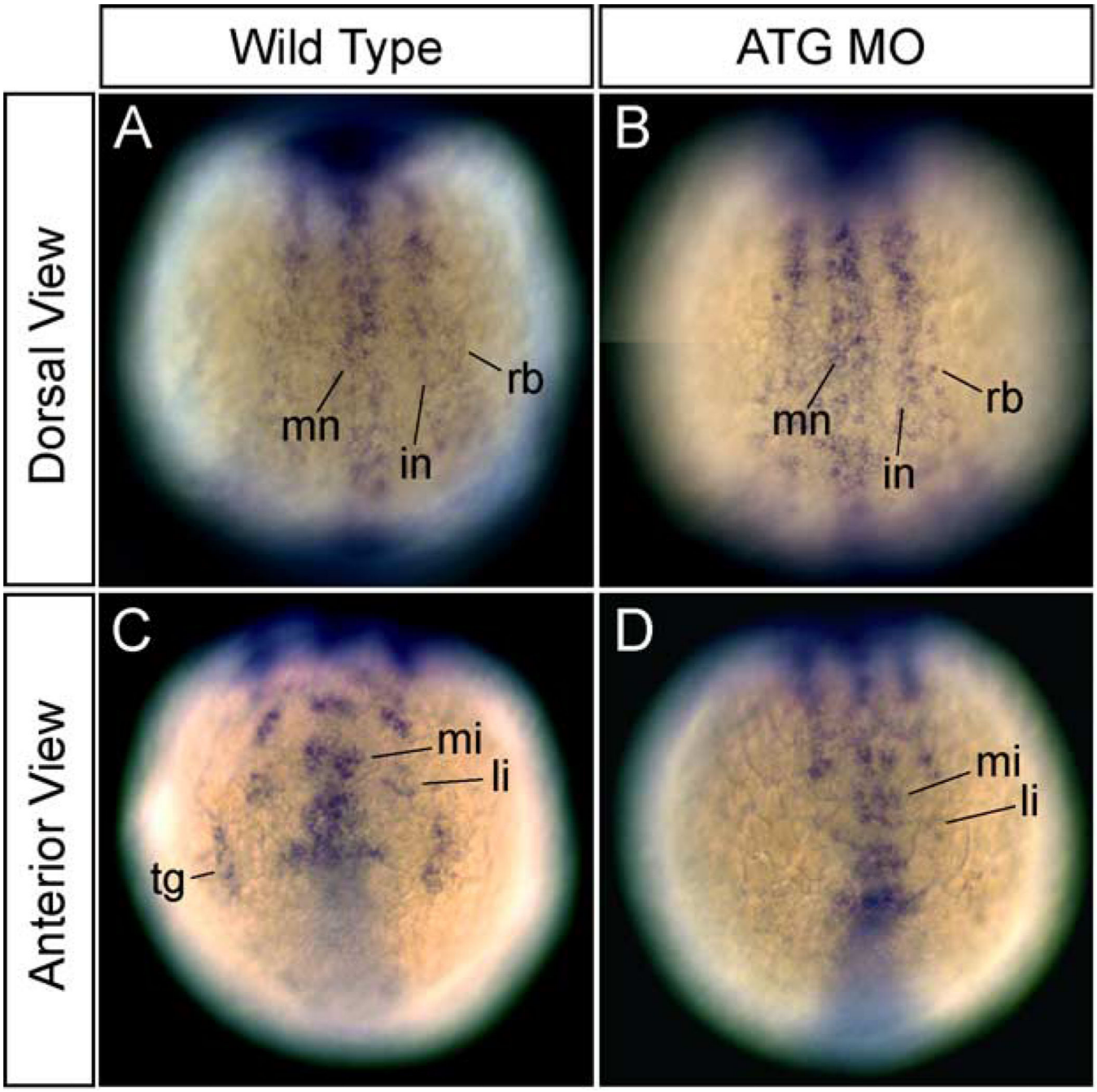

Fig. 7.

Expression of the upstream gene, *neurogenin1*, for *HuC*, *tlx3a*, and *neuroD* marking RB neurons and neurons in the trigeminal placodes, in embryos injected with *dlx3b*-MO and *dlx4b*-MO at 3-somite stage. (A and C) Wild-type embryos. (B and D) 20 ng ATG-*dlx3b*-MO/20 ng ATG-*dlx4b*-MO-injected embryos. (A and B) The expression of *neurogenin1* in RB neuron precursors (rb) is normal in MO-injected embryos. Dorsal views. (C and D) The expression of *neurogenin1* in the precursors of neurons in the trigeminal placodes (tg) is absent in MO-injected embryos (D). Anterior views. mn, primary motor neuron precursors;

in, primary interneuron precursors; mi, anterior medial hindbrain interneuron precursors; li, anterior lateral hindbrain interneuron precursors.

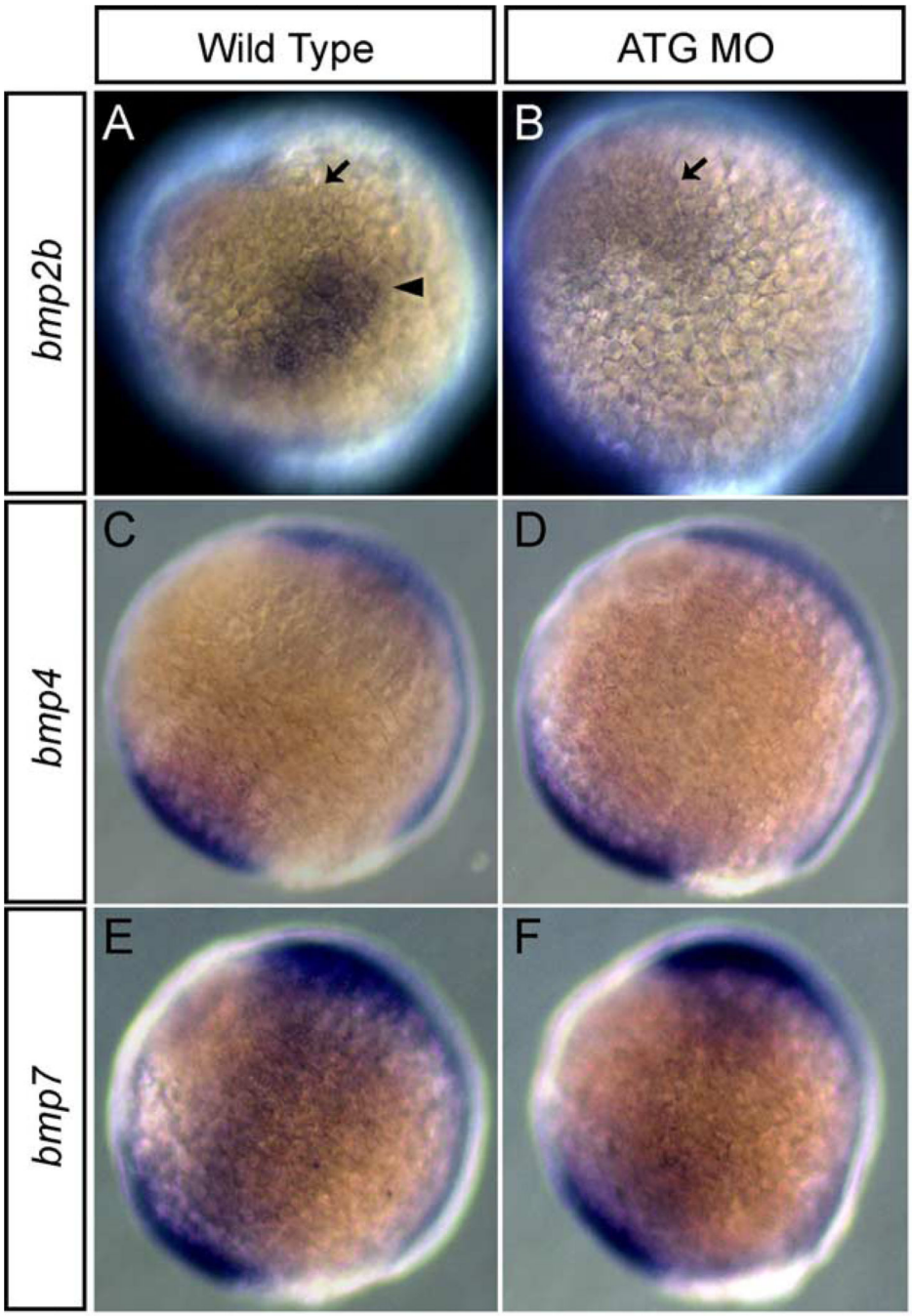

Fig. 8.

Expression of *bmp2b*, *4*, and *7* in embryos injected with *dlx3b*-MO and *dlx4b*-MO at 90% epiboly. Expression in wild-type embryos of *bmp2b* (A), *bmp4* (C), and *bmp7* (E). Expression in 20 ng ATG-*dlx3b*-MO/20 ng ATG-*dlx4b*-MO-injected embryos of *bmp2b* (B), *bmp4* (D), and *bmp7* (F). (A and B) show that there is a strong triangle of *bmp2b* expression (arrowhead) at the border of the non-neural ectoderm in the wild-type embryos but this region is lost in MOs-injected embryos. Ventral *bmp2b* expression persisted in MOs-injected embryos (arrow). No alterations are seen in the expression of *bmp4* and *bmp7*

between wild-type embryos and MOs-injected embryos (C–F). Lateral views, and dorsal is to the right.

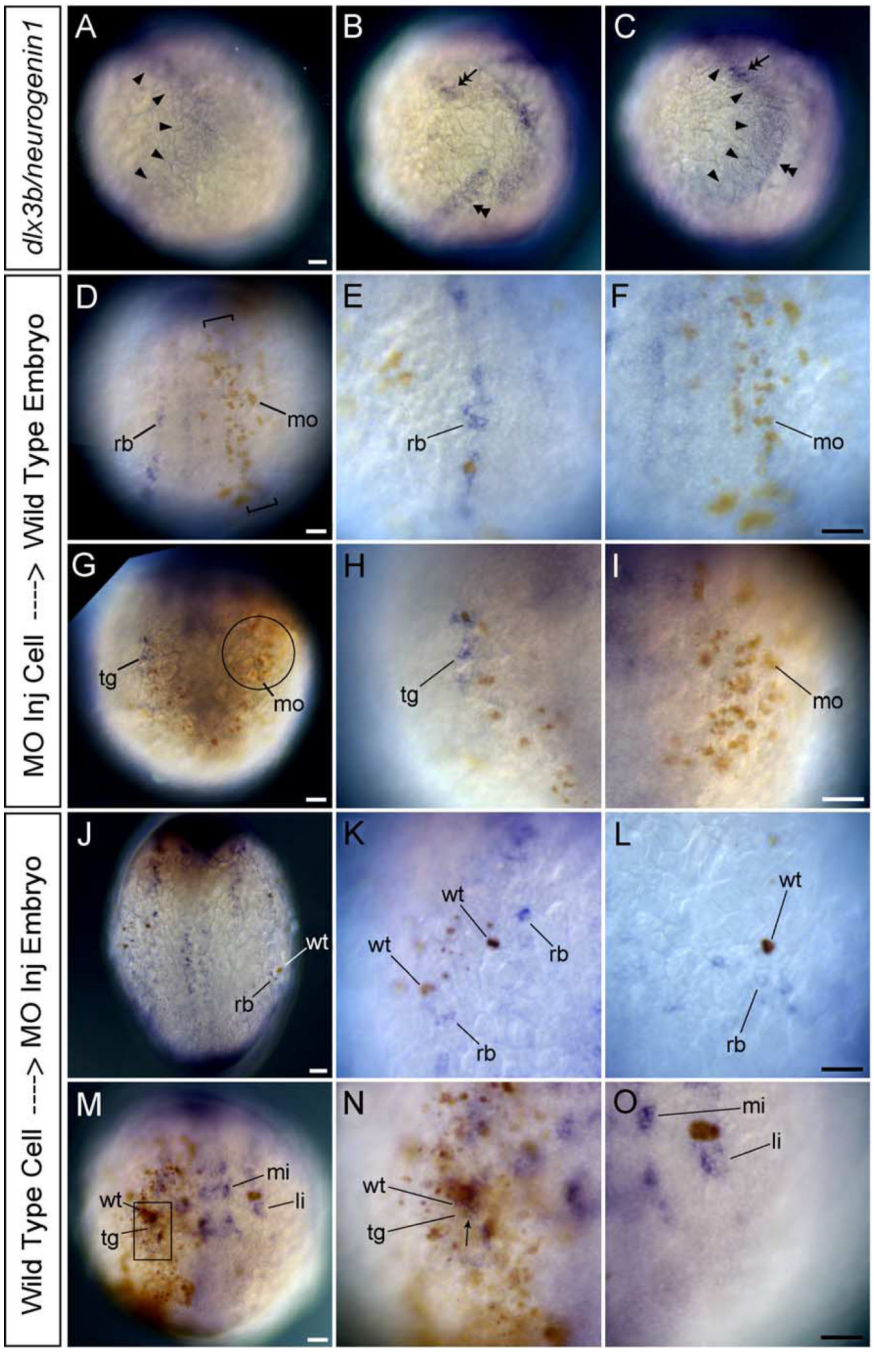

Fig. 9.

HuC expression in mosaic embryos between wild-type and MO-injected embryos. (A–C) Wild-type embryos at tailbud stage. Lateral views, and dorsal is to the right. (D–O) Transplanted embryos at 3-somite stage. (D–I) are the wild-type host embryos. (J–O) are the MOs-injected host embryos. (D and J) Dorsal views. (G and M) Anterior views. (A) Expression pattern of *dlx3b* (arrowheads). (B) Expression pattern of *neurogenin1* (double arrowhead in the trunk and double arrow in the head). (C) Expression pattern of *dlx3b* and *neurogenin1*. (D–O) *HuC* expression in mosaic embryos. (A–C) show that *dlx3b* expression

(arrowheads) and *neurogenin1* expression in the lateral trunk (double arrowhead) are adjoining but not overlapping in the trunk. In contrast, *dlx3b* expression and *neurogenin1* expression in the lateral head (double arrow) are overlapping. (D–F) show that RB neurons (rb) do not develop in the neural plate where brown-labeled MOs-injected cells (mo) are in a narrow region (bracket) just outside the neural plate. *dlx3b* and *dlx4b* should be expressed in this narrow region under wild-type conditions. (E) A high magnification view of RB neurons (rb) on the left side of embryo in D. (F) A high magnification view of the narrow region defined by brackets on the right side of embryo in D. The high number of MO-injected cells (brown, mo) is able to inhibit *HuC* expression in neighboring cells. (G–I) show that neurons in the trigeminal placodes (tg) do not develop there when brown-labeled MOs-injected cells occupy the trigeminal placode (circle). *dlx3b* and *dlx4b* are expressed in this circle region under wild-type conditions. (H) A high magnification view of neurons in the trigeminal placode (tg) on the right side of embryo in G. (I) A high magnification view of the trigeminal placodal region defined by the circle on the left side of embryo in G. The high number of MO injected cells (brown, mo) is able to inhibit *HuC* expression in the trigeminal placode. (J–L) In a MO-injected background, RB neurons are seen only around the brown-labeled wild-type cells (wt) in the embryonic epidermis. The host MOs-injected embryos develop no or reduced levels of RB neurons. (K) A high magnification view of RB neurons on the left side of embryo in J. RB neurons can be seen only around the brown wild-type cells (wt). (L) A high magnification view of RB neurons on the right side of embryo in J. RB neurons can be seen only around the brown wild-type cells (wt). (M–O) Neurons in the trigeminal placodes develop when brown-labeled wild-type cells occupy the trigeminal placode (square) in the host MO-injected embryos having no trigeminal placodal neurons. (N) is the high magnification view of the trigeminal placode defined by the square on the right side of embryo in M. The high number of wild-type cells expresses *HuC* in themselves, so many double-labeled neurons can be seen in the trigeminal placode (arrow). (O) A high magnification view of the trigeminal placodal region on the left side of embryo in M. No neurons in the trigeminal placode are observed where wild-type cells are not present. li, anterior lateral hindbrain interneuron; mi, anterior medial hindbrain interneuron. All scale bars, 50 μm. Scale bar in A applies for A, B, and C. Scale bar in F applies for both E and F, etc.

Dev Biol. Author manuscript; available in PMC 2014 May 20.

Table 1

dlx3b/dlx4b MO effects in zebrafish[a]

Injection	Amounts (ng/embryo)	*N*	Phenotype (reduced or absent)		Defective gastrulation[c]	Dead[c]
			RBs	TG[b]		
Control	40	38	0	0	–	–
MO		108	–	–	0	7
dlx3bhd–	0.150–0.200	40	18	–	ND	ND
EnR		44	–	14		
dlx3b/dlx4b	40	109	52	–	–	–
ATG–		73	–	39	–	–
MO		273	–	–	17	22
dlx3b/dlx4b	40	56	32	–	–	–
E2I2–		51	–	38	–	–
MO		97	–	–	5	11
dlx3b/dlx4b	40					
ATG–		30	4[d]	ND	ND	ND
MO+	0.150					
dlx3bhd–						
VP16						

ND is not done.

[a] All sets of injection experiments were done at least three times.

[b] RB = Rohon–Beard sensory neuron, TG = Trigeminal ganglia placode.

[c] Checked at the 3-somite stage.

[d] We have defined reduced to have 12 or less RB neurons/per embryo. This is the average number of total RB neurons in the MO-injected embryos (see Table 3).

Table 2

Dose effects of dlx3b/dlx4b MO[a]

Injection	Amounts (ng/embryo)	*N*	Phenotype (reduced or absent)	
			RBs	TG[b]
dlx3b/dlx4b	8 + 8	14	7	7
ATG-MO	16 + 16	23	8	10
dlx3bhd-EnR	0.060	20	13	14
	0.120	19	15	13

[a] All sets of injection experiments were done at least two times.

[b] RB = Rohon-Beard sensory neuron, TG = trigeminal ganglia placode.

Table 3

Rescue effect of dlx3bhd-VP16 on the numbers of RB neurons[a]

Injection	Amounts (ng/embryo)	*N*	Average number of RB neurons[b]		
			Left	Right	Total
Uninjected	NA	31	18.5	19.0	37.5 ± 4.2
dlx3b/dlx4b E2I2-MO	40	20	6.5	6.2	12.7 ± 3.7
dlx3b/dlx4b ATG-MO	40	20	6.6	5.7	12.3 ± 3.7
dlx3b/dlx4b ATG-MO+ dlx3bhd–VP16	40 0.150	30	10.3	11.3	21.6 ± 7.1

[a] All sets of injection experiments were done at least three times.

[b] The number of Rohon-Beard sensory neurons (RB) were counted on each side of a 3-somite-stage embryo, visualized with HuC in situ hybridization.